PERGAMON

Deep-Sea Research I 48 (2001) 1139–1168

DEEP-SEA RESEARCH
PART I

www.elsevier.com/locate/dsr

Physical and biological modeling in the Gulf Stream region Part II. Physical and biological processes

Laurence A. Anderson*, Allan R. Robinson

Division of Engineering and Applied Sciences, Harvard University, Cambridge, MA 02138, USA

Received 12 May 1998; received in revised form 4 October 1999; accepted 31 October 2000

Abstract

Mesoscale physical and biological processes are examined at the Gulf Stream front by means of a 4-D simulation including physical and biological data assimilation. The data assimilated are from Leg 1 of the Fall BIOSYNOP cruise, 21 Sept.–8 Oct. 1988, and GULFCAST data for the same period. Focus is on the vertical velocities at the front, the vertical and horizontal transports of nutrients and plankton, and the impact of these transports on phytoplankton biomass, production and organic particle export. It was found that while jet meandering enhances new production at the front, primary production and phytoplankton concentration at the front are not significantly enhanced over those of Slope water. Winds during this period also have little impact on productivity at the front, due to their high temporal variability. Ring–stream interactions, however, significantly increase the net vertical and meridional transports of nutrients and plankton and can lead to phytoplankton patchiness at the front. This emphasizes the importance of submesoscale events between interacting mesoscale physical features in the transport of nutrients and plankton, and in explaining the observations. The enhanced phytoplankton concentrations observed during BIOSYNOP are found to be primarily due to advection (convergence) rather than in situ biological growth.

Keywords: Data assimilation; Gulf Stream; Modeling; Physical–biological interactions; Nitrogen cycle

1. Introduction

Enhanced phytoplankton concentrations have often been observed at open ocean fronts (e.g. Owen, 1981; Lutjeharms et al., 1985; Yamamoto et al., 1988; Heilmann et al., 1994; Claustre et al., 1994). In some cases, the enhanced concentrations are due to advective processes and in other cases

* Corresponding author. Present address: Woods Hole Oceanographic Institution, Woods Hole, MA 02543, USA.
E-mail address: landerson@whoi.edu (L.A. Anderson).

0967-0637/01/$ - see front matter
PII: S0967-0637(00)00092-3

in situ biological growth. Alterations in trophic structure and particle export have also been observed at fronts (Le Fèvre and Frontier, 1988; Prieur and Sournia, 1994) suggesting significant local modifications in nutrient recycling.

This study, the second of two parts (see Anderson et al., 2000), examines the mesoscale physical processes associated with the Gulf Stream front, the associated vertical and horizontal transports of nutrients and plankton, and the impact of these transports on phytoplankton biomass, production and organic particle export. It has been theorized that at the Gulf Stream front the large vertical velocities due to stream meandering (Hitchcock, 1988; Woods, 1988; Flierl and Davis, 1993), diffusive isopycnal mixing (Olson et al., 1994) and enhanced diapycnal mixing (Pelegri and Csanady, 1994) may both increase the upward transport of nutrients and lift phytoplankton cells to higher light intensities, resulting in enhanced primary productivity.

Interestingly, however, enhancement in phytoplankton is often not observed at the Gulf Stream front (e.g. Fig. 2 of Hitchcock, 1988). Surface ocean color images indicate that the Gulf Stream is primarily a boundary between the oligotrophic Sargasso waters to the south and more productive Slope waters to the north; phytoplankton enhancement is seen sometimes along the front, but not always everywhere (see Coastal Zone Color Scanner (CZCS) data at http://daac.gsfc.nasa.gov/). Transects across the Gulf Stream during the BIOSYNOP/Anatomy of a Meander cruise (Lohrenz et al., 1993; Hitchcock et al., 1993; Mariano et al., 1996) had mixed results. The cross sections generally showed no local maxima in chlorophyll at the Gulf Stream front, although enhanced Chl concentrations were found downstream of a meander crest during the fall cruise. It was unclear whether the patch was due to physical or biological processes, and whether the ultimate source was the meandering processes or a nearby ring–stream interaction. The rapid downstream flow in the Gulf Stream (approx. 100 km/d), coupled with the lag time in phytoplankton response to increased nutrients (Flierl and Davis, 1993), makes it difficult to ascertain from the data which variations in phytoplankton concentrations are linked to which physical processes. A further complication is that phytoplankton can be advected off the continental shelf and into the Gulf Stream (Lillibridge et al., 1990), which may be a source of observed phytoplankton patches. Because of this difficulty in interpreting the observations, the Gulf Stream is an excellent testbed for using models to determine the relationships between specific physical processes and the corresponding responses of primary producers. Understanding the links between physical and biological processes in the Gulf Stream should give us insight into the processes controlling biological distributions at other fronts as well.

Because of the complexity of the physical processes and the biological responses in the Gulf Stream, we use a time-dependent, three-dimensional, physical–biological model. Physical and biological data assimilation is used to keep the simulation consistent with data. As such, the model can be viewed as an interpolator that synthesizes all the various physical, biological and meteorological observations with each other and with physical and biological principles (i.e. the model equations), and that makes best estimates where data is not available.

Our goal was to make the best possible reconstruction of the physical–biological state of the Gulf Stream and its processes during the 1988 Fall BIOSYNOP cruise, in order to discern the dominant physical and biological processes and their relationships as indicated by the consensus of the various data types. The specific objectives were (1) to determine what physical or biological processes caused the high phytoplankton patch at the front observed during Fall BIOSYNOP, and (2) to assess the impact of stream meandering, ring–stream interactions and winds on vertical

velocity, vertical NO_3 transport, phytoplankton and zooplankton patchiness, primary production, new production, particle export, and the cross-stream exchange of NO_3 and phytoplankton.

Comparison of our simulation results with previous, idealized modeling studies of physical–biological interactions at fronts will be made in Section 4. This study illustrates the important impact of three-dimensional processes and submesoscale interactive events on physical–biological interactions, thereby demonstrating that realistic, high-resolution 4-D field estimation may often be necessary to capture the essential physical–biological interactions that explain the data.

In this study we synthesize information from two main data sets, the combined Fall BIOSYNOP/Anatomy of a Meander data set and the GULFCAST data set, described in Anderson et al. (2000). We concentrate on a specific 17-day time period, 21 Sept.–6 Oct. 1988, which is Leg 1 of the Fall BIOSYNOP experiment, when nutrient-limited conditions typical of late summer were prevalent. It was expected that the biological response to upward nutrient transport would be most significant during such strong nutrient limitation. Leg 2 of BIOSYNOP encountered higher surface density values, higher surface NO_3 concentrations, and higher primary production in Slope waters (Lohrenz et al., 1993), indicative of enhanced mixing from below.

2. The model

The physical and biological models used in this study are described in detail in Anderson et al. (2000). The physical model is a primitive equation model with 15 km horizontal resolution and 30 vertical levels. The biological model is of the nitrogen cycle and has five state variables: nitrate, ammonium, phytoplankton, zooplankton, and non-sinking (suspended particulate and dissolved) organic nitrogen. These are advected and diffused in the three-dimensional flow field and subject to biological source and sink terms. Fast-sinking detritus is also included in the model, but does not have an explicit distribution, i.e. it sinks and remineralizes instantaneously.

Physical–biological initialization and assimilation fields based on data are constructed for 28 Sept. and 5 Oct. 1988, by the method described in Anderson et al. (2000). Assimilation into the simulation is done by means of an optimal interpolation scheme (Lozano et al., 1996), with one assimilation timestep per day. Assimilation weights vary from values of 100% in places where data have been melded into the assimilation field, decreasing to weights of 50% where there is no data and the assimilation field is based on a feature model estimate. In addition assimilation weights are multiplied by a factor that linearly increases on the 3 d preceding the date of the assimilation field (5 Oct.), to allow a smooth melding of the assimilation field into the simulation. See Anderson et al. (2000) for more details.

Data assimilation is essential to ensure that the simulations are the best possible reconstruction of the observed physical–biological state of the Gulf Stream during BIOSYNOP. It is important that physical–biological simulations be rigorously validated with data. The ocean ecosystem is a complex web, such that there is considerable uncertainty in the number of biological state variables necessary to describe the system. Simple biological models may not capture all the important processes, while complex models rely on unobserved state variables. Biological initial conditions, boundary conditions, parameterizations and parameter values are generally poorly known. Slightly different biological parameterizations can lead to different results (Haney and Jackson, 1996). Both the physical and biological dynamics are non-linear, and can have chaotic

behavior. The dominant physical–biological coupling may rely on the non-linear terms, e.g. biological production strongly responds to vertical velocities caused by non-linear physical processes. The predictive skill of biological models, particularly regarding their response to physical processes, is likely to be sensitive to all of these uncertainties. Modeling "process" studies that lack rigorous validation with data are largely speculative and, as discussed in Section 4, can result in incomplete explanation of the data and incorrect or inconclusive identification of the primary physical–biological interactions. It is generally very difficult to devise a simulation that agrees adequately with all the data, without some sort of data assimilation to correct for imperfect dynamics or lack of information.

In our simulations the initial conditions, parameter values and parameterizations were carefully tuned so that the simulation assimilates the data with little generation of spurious discontinuities or oscillations in the physical or biological fields. The fact that the data assimilate in smoothly in the last half of the simulation indicates that the evolution of the entire simulation is fairly accurate and the dynamics reasonable. Comparison was also made with simulations without data assimilation, to further evaluate the dynamical processes. By these rigorous means we were able to obtain simulations in agreement with the various data types, from which we can draw conclusions as best one can about the physical–biological interactions that occurred during BIOSYNOP.

3. Description of simulations

Runs 1 through 5 (Table 1) were methodological tests discussed in Anderson et al. (2000). Run 6, discussed in Section 3.1, is our best estimate of Gulf Stream processes in the absence of winds. Run 7 (Section 3.2) includes realistic wind forcing and an active mixed layer depth to explore the influence of winds. Run 8 (Section 3.3) examines the effect of meanders versus ring–stream interactions. Because the model grid is rotated 22° to the northeast, locations below are given in (i,j) grid coordinates rather than latitude and longitude.

Table 1
Model simulations

Run	Start day	Fields[a]	Rings[b]	Assimilation[c]	Wind forcing[b]
1	272	FM	Y	N	N
2	279	FM	Y	N	N
3	272	FM	Y	P	N
4	272	FM	Y	B	N
5	272	FM	Y	P + B	N
6	272	FM + data	Y	P + B	N
7	272	FM + data	Y	P + B	Y
8	279	FM	N	N	N

[a] FM = feature model fields, dynamically adjusted; FM + data = feature model fields with data melded in and dynamically adjusted.
[b] Y = yes; N = none.
[c] P = physical data assimilation; B = biological data assimilation; N = none.

Due to the lack of NH_4, DON, detritus and particle flux observations for model verification, particularly in Slope waters, the quantitative model results regarding these fields are somewhat speculative. Emphasis in this study is placed on physical processes and the nitrate and phytoplankton results.

3.1. *Run 6*: *Gulf Stream processes without winds*

Run 6 is our best estimate of the effects of the Gulf Stream processes in the absence of external forcing (winds). Run 6 begins on 28 Sept. and is run for 10 d (until 8 Oct.). The 5 Oct. field estimate is assimilated on days 4 through 7 of the simulation.

3.1.1. *Temperature and horizontal velocity*

During this period two warm core rings (Fig. 1a, centered at $i = 34$, $j = 42$ and $i = 52$, $j = 40$) and two cold core rings ($i = 16$, $j = 22$ and $i = 40$, $j = 12$) were near the Gulf Stream in this region. The cold-core rings have warm surface signatures due to Gulf Stream water. The BIOSYNOP observations centered around the meander crest at ($i = 30$, $j = 34$), which was strongly interacting with the western warm core ring; the ring was in the process of being absorbed back into the Gulf Stream (Anderson et al., 2000, Fig. 4). The meander trough at ($i = 42$, $j = 25$) was steepening, and was observed to pinch off as a ring around 17 Oct. (model day 19). The eastern cold-core ring at ($i = 40$, $j = 12$) in the model starts interacting with the Gulf Stream on day 2, and by day 10 a warm

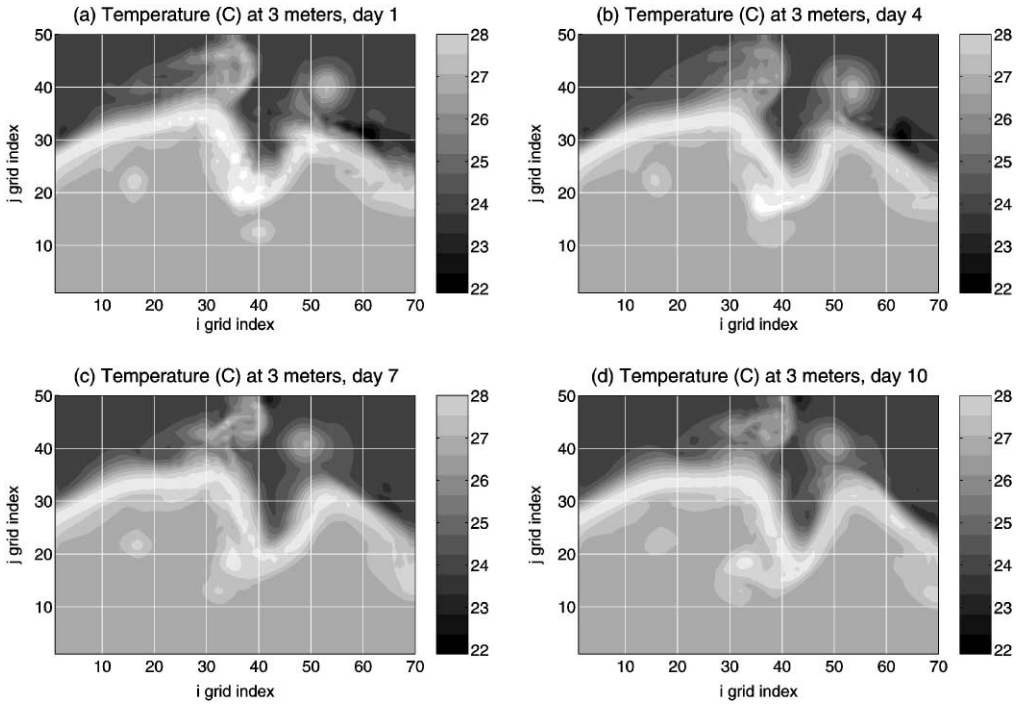

Fig. 1. Temperature in Run 6. *X* and *Y* axis values are grid point indicies. The model grid has 15 km spacing. The domain is rotated 22° (see Anderson et al., 2000), such that the latitude and longitude of these indicies vary.

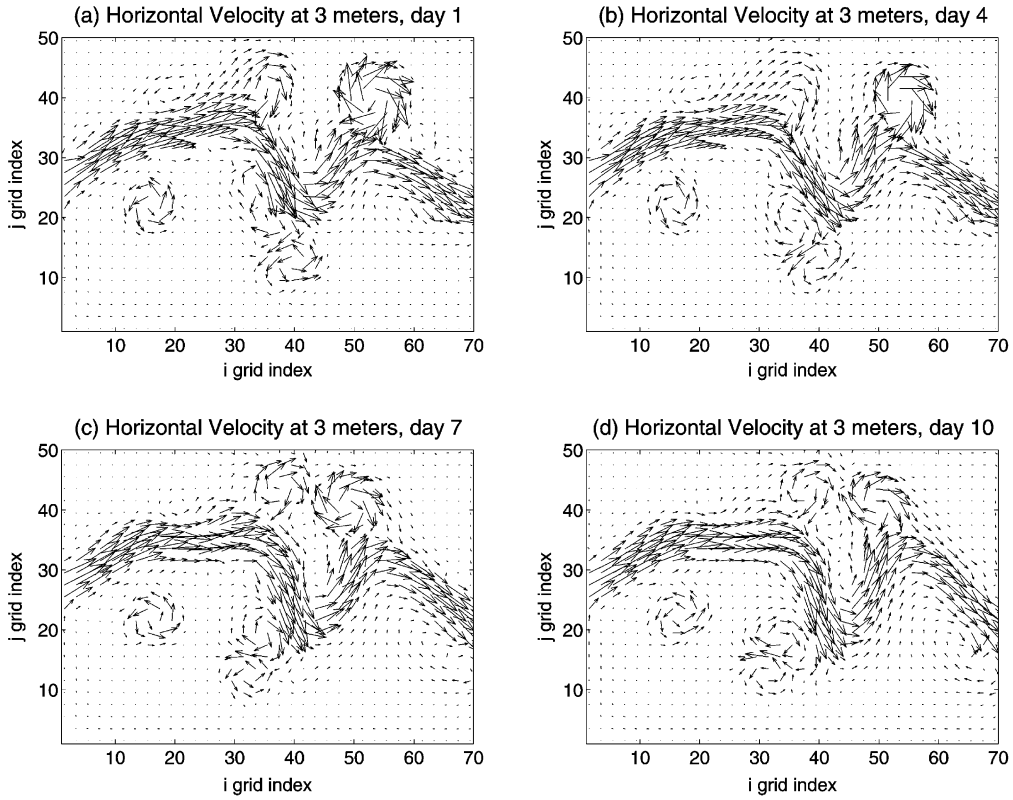

Fig. 2. Horizontal velocity vectors in Run 6. Maximum values are 160 cm/s.

streamer has been detached, consistent with the NOAA/NOS Oceanographic Analysis of AVHRR data for 5 Oct. 1988 by Jenifer Clark. This temperature reconstruction (Fig. 1) is our best estimate based on the BIOSYNOP and GULFCAST data sets.

Horizontal velocities on level 1 (Fig. 2) reach up to 160 cm/s at the Gulf Stream axis, as observed (Halkin and Rossby, 1985). Velocities are low in the artificially homogeneous regions away from the Gulf Stream and rings.

3.1.2. Vertical velocity

During BIOSYNOP, horizontal divergence (upwelling) was observed upstream of the meander crest and horizontal convergence (downwelling) downstream, based on the vertical displacement of isopycnals and the subsurface chlorophyll maximum (Lohrenz et al., 1993; Hitchcock et al., 1993), POGO trajectories (Hitchcock et al., 1993), ADCP data (Liu and Rossby, 1993) and zooplankton species abundance (Ashjian, 1993). This is consistent with previous theory and observations of meanders (Osgood and Bane, 1987; Bower and Rossby, 1989; Onken, 1992; Yoshimori, 1994; Olson et al., 1994; Lindstrom and Watts, 1994; Lindstrom et al., 1997) with upwelling approaching anticyclonic excursions and downwelling approaching cyclonic excursions, in accord with vorticity conservation and vortex stretching (Levine et al., 1986; Woods, 1988).

The simulated vertical velocities agree well with these observations (Fig. 3). (See Section 3.3 for vertical velocity patterns in more idealized simulations.) Upwelling occurs upstream of the crest (e.g. on day 4 at $i = 29$, $j = 38$) and downwelling downstream ($i = 36$, $j = 36$); likewise downwelling occurs upstream of the meander trough ($i = 40$, $j = 22$) and upwelling downstream ($i = 46$, $j = 29$). The patterns, however, are complex and transient near the ring–stream interactions. The highest vertical velocities at 42 m are around 15 m/d, associated with the intense central trough at ($i = 40, j = 22$) due to its small radius of curvature, and with the ring–stream interactions (e.g. at $i = 36, j = 36$ on day 4). Weaker velocities are associated with minor meanders (e.g. $i = 19$, $j = 33$). Rings in isolation (e.g. $i = 18, j = 21$) have even lower vertical velocities (< 2.5 m/d at this depth).

On day 7 small-scale variability and enhanced values are generated due to the assimilation of the high-resolution data (Fig. 3c). These spurious vertical velocities however quickly dissipate as waves (essentially gone by day 10) and do not greatly affect the other physical or biological fields. For example, new production on day 7 is 5.6% higher in Run 6 than in an identical run without data assimilation; thus the impact of the waves on new production is small.

Vertical velocities increase in magnitude with depth to extrema between 300 and 900 m. Maximal vertical velocities at depth are in the vicinity of 100 m/d. This agrees well with estimates from current meters, inverted echo sounders and RAFOS floats of 1–2 mm/s = 86–173 m/d for typical meanders (Lindstrom and Watts, 1994), although on rare occasion vertical velocities up to 4–6 mm/s have been observed (Lindstrom et al., 1997; Hummon et al., 1991).

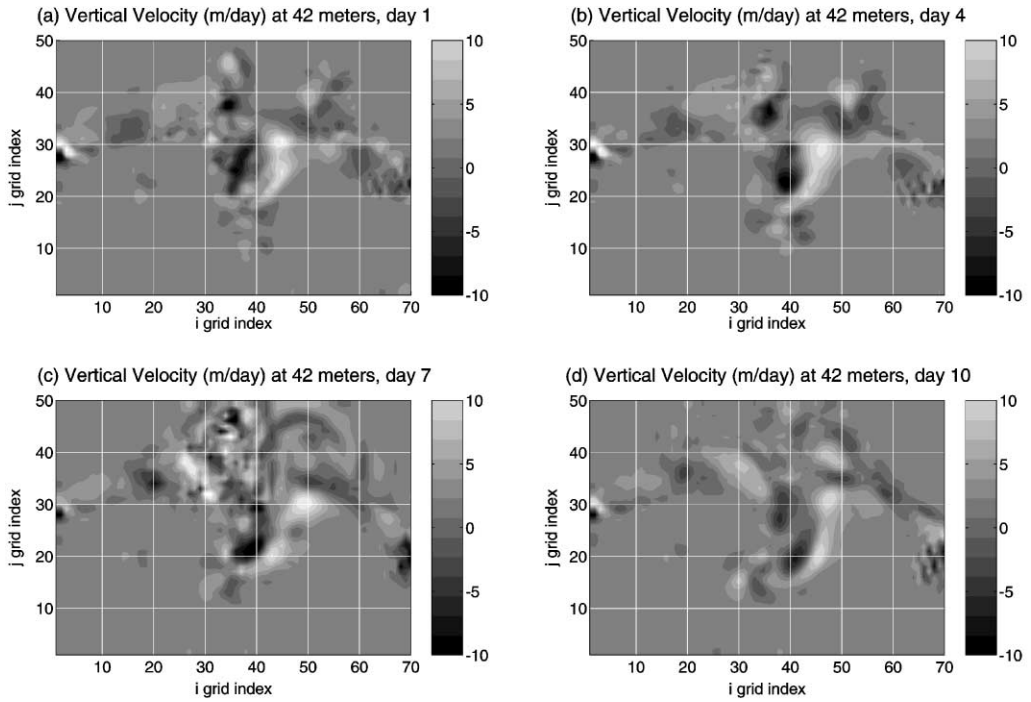

Fig. 3. Vertical velocity at 42 m in Run 6. Negative values indicate downward velocities.

The vertical velocities due to meandering and ring–stream interactions are much greater than any general upwelling on the southern side and downwelling on the northern side of the front hypothesized by two-dimensional models (Bleck et al., 1988; Pollard and Regier, 1992). The meander downwelling zones in our simulations contribute to subduction at the front (Spall, 1995), which likely explains the patchy nature of observed high subsurface biomass concentrations (Pollard and Regier, 1992). Our simulation was not long enough to investigate the long-term effects of the subduction process.

3.1.3. Nitrate

The biological fields change little qualitatively and quantitatively during Run 6 apart from changes in stream axis position. Therefore, for brevity, only the biological fields on day 4 will be shown. Day 4 was chosen partly to avoid any possible spurious effects due to the data assimilation.

Nitrate on level 1 (Fig. 4a) is highest in the center of the trough. This does not correspond with an upwelling location; it is at the center of a recirculation gyre (Dutkiewicz et al., 1993; Bower, 1991), even though the circulation is not completely closed (Fig. 2b). The high NO_3 patch is due to mixing up of NO_3 from the base of the mixed layer, which is due to horizontal detrainment of upwelled water from the Gulf Stream. In Slope waters, NO_3 has a mottled appearance because the nutricline is at the base of the mixed layer; variations in the sign of vertical advection inject nutrients into the mixed layer. In the Sargasso this does not occur because the mixed layer depth (30 m) is much less than the nutricline depth (80 m). In these simulations mesoscale eddies are absent in Slope and Sargasso waters, which would enhance patchiness (McGillicuddy and Robinson, 1997). As even the highest NO_3 values are in the nanomolar range, NO_3 is essentially depleted at the sea surface throughout the entire domain.

BIOSYNOP NO_3 observations show surface values in Slope waters near the meander crest of 0.03 μM. This is higher than estimated in Run 6, but similar to Run 7 (0.02 μM), when winds are included (Section 3.2). In the Sargasso, model NO_3 and NH_4 values at the sea surface are 0.2 and 5 nM, respectively, not far from observed (approx. 1 and 10 nM for NO_2 and NH_4; Brzezinski, 1988).

3.1.4. Phytoplankton

Phytoplankton at the sea surface (Fig. 4b) are slightly enhanced in the center of the trough recirculation gyre, consistent with previous theory and observations (Bower, 1991; Dutkiewicz et al., 1993; Olson et al.,1994). As with NO_3, surface phytoplankton are not correlated with upwelling, but are high due to vertical mixing from below, where phytoplankton are enhanced due to growth (in response to the elevated NO_3 concentration) and due to horizontal advection from the Gulf Stream subsurface Chl maximum.

Local maxima in vertically integrated phytoplankton (Fig. 4c) occur on the Slope side of the Gulf Stream axis. Rather than being correlated with upwelling, as was expected from upwelling of

Fig. 4. Biological fields on day 4 of Run 6. Vertical integration is over the upper 278 m, although plankton concentrations and production are generally negligible below 150 m. A C/N ratio of 6.625 mol/mol was used to convert from N to C (Redfield et al., 1963). The white contour is the location of the 15 C isotherm at 200 m, which approximates the location of the North Wall separating Gulf Stream and Slope waters. Solid (dashed) black contours indicate where upward (downward) vertical velocity at 42 m exceeds 2 m/d.

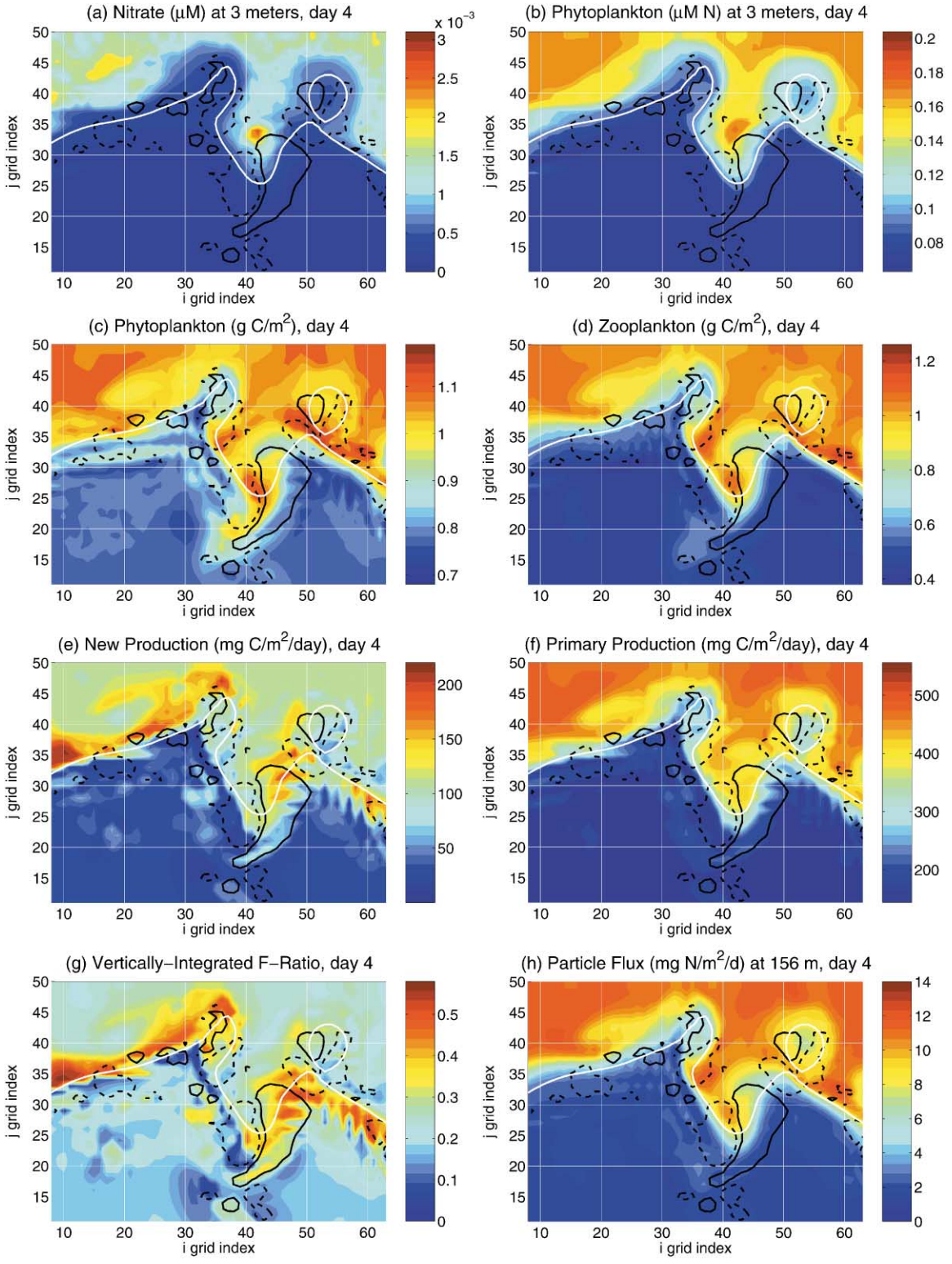
(a) Nitrate (μM) at 3 meters, day 4
x 10^-3
3
2.5
2
1.5
1
0.5
0
(b) Phytoplankton (μM N) at 3 meters, day 4
0.2
0.18
0.16
0.14
0.12
0.1
0.08
(c) Phytoplankton (g C/m^2), day 4
1.1
1
0.9
0.8
0.7
(d) Zooplankton (g C/m^2), day 4
1.2
1
0.8
0.6
0.4
(e) New Production (mg C/m^2/day), day 4
200
150
100
50
(f) Primary Production (mg C/m^2/day), day 4
500
400
300
200
(g) Vertically–Integrated F–Ratio, day 4
0.5
0.4
0.3
0.2
0.1
0
(h) Particle Flux (mg N/m^2/d) at 156 m, day 4
14
12
10
8
6
4
2
0
i grid index
j grid index
10
20
30
40
50
60
15
20
25
30
35
40
45
50

nutrients or lifting of phytoplankton into higher light regimes, the phytoplankton maxima are immediately downstream of downwelling (convergence) zones. The enhanced values essentially occur at 61 m (level 8) and below, and are primarily due to advection rather than biological growth; convergence and downwelling collects and pushes the phytoplankton deeper in the water column, increasing the vertical integral. The low values upstream of the meander crest at ($i = 29, j = 38$) and high values downstream at ($i = 36, j = 35$) are consistent with the BIOSYNOP observations on days 271–285 (Lohrenz et al., 1993; Hitchcock et al., 1993; Olson et al., 1994; Mariano et al., 1996). The data transects (Lohrenz et al., 1993; Hitchcock et al., 1993) agree with the model that, even though the maximum Chl concentrations are lower downstream of the crest than upstream, vertically integrated Chl is higher because the Chl maximum resides deeper in the water column. Low observed production values downstream of the crest also indicate that the high phytoplankton concentrations there must not be due to growth (Lohrenz et al., 1993; Ashjian et al., 1994). Thus the data and model agree that the phytoplankton maximum found downstream of the meander crest during BIOSYNOP was primarily due to advective processes rather than growth.

A phytoplankton cross section (Fig. 5) shows subsurface phytoplankton biomass maxima at 76 m in Sargasso waters and at 37 m in Slope waters, i.e. at the top of the respective nutriclines. Higher values occur in the Slope. This is supported by the BIOSYNOP Chl observations (Lohrenz et al., 1993; Hitchcock et al., 1993). Although the relationship between Chl and biomass is not straightforward (Longhurst and Harrison, 1989), the existence of subsurface *biomass* maxima are supported in that the increase in Chl with depth at the Chl maxima (see Fig. 9 in Anderson et al., 2000) is much greater than the increase in the Chl/C ratio with depth (Malone et al., 1993). Subsurface biomass maxima have been observed in other oligotrophic regions (e.g. Gould and Wiesenburg, 1990; Furuya, 1990). At 80 m depth, higher phytoplankton concentrations are observed in the Sargasso than in the Slope due to self-shading in the latter. The phytoplankton concentrations in Slope and Sargasso waters agree well with observations (Anderson et al., 2000).

Near the front, subsurface Chl patches are often observed in downwelling zones but not upwelling zones (Lohrenz et al., 1993; Hitchcock et al., 1993). This is also true in the model (e.g. Fig. 5 at $j = 37$, 50 m depth) although there are exceptions, even in idealized simulations

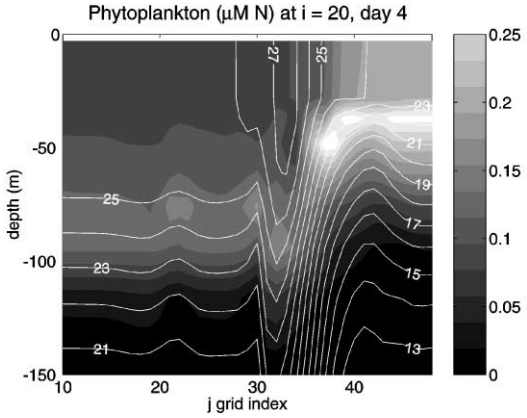

Fig. 5. Meridional cross section of phytoplankton biomass in Run 6. Temperature contours are given at 1°C intervals. X axis values are j indicies, with Sargasso waters to the left of $j = 38$ and Slope waters to the right.

(Section 3.3) due to the complexity of the evolving 3-D fields. Subsurface maxima at the front may or may not constitute vertically integrated maxima, depending on the overlying waters, which are generally less productive than Slope water.

3.1.5. Zooplankton

During BIOSYNOP, zooplankton concentrations measured by net tows did not show any significant meander-related enhancement (Ashjian et al., 1994). Zooplankton concentrations measured by ADCP (i.e. large zooplankters) however were enhanced downstream of the meader crest (Ashjian et al., 1994; Olson et al., 1994; Mariano et al., 1996). The center of the zooplankton patch appeared to be approximately 50 km downstream of the center of the phytoplankton patch, although this may have been due to the fact that zooplankton were sampled approximately 1 week later than phytoplankton (Mariano et al., 1996). Because 50 km is about half a day in advective time, the zooplankton patch was considered unlikely to be due to growth based on grazing of phytoplankton; large zooplankton would need a longer time to increase their biomass (Ashjian et al., 1994; Olson et al., 1994). This suggests the zooplankton patch must have been primarily due to advective processes (i.e. convergence/downwelling), possibly in combination with vertical migration (Franks, 1992).

Our simulation yields zooplankton distributions (Fig. 4d) similar to phytoplankton, with a maximum downstream of the meander crest as observed. This maximum is due primarily to convergence/downwelling, i.e. the same physical process that increases phytoplankton there. Our simulation shows general correlation between the phytoplankton and zooplankton anomalies, in agreement with the data.

Lowest zooplankton concentrations during BIOSYNOP were found at the apex of the meander crest (Ashjian et al., 1994; Olson et al., 1994; Mariano et al., 1996), which was conjectured to be due to dilution from the upwelling/divergence upstream. Our simulation also yields low values at the crest apex, and suggests they are instead due to the presence and entrainment of the warm core ring to the north.

Model zooplankton concentrations in the Sargasso (433 mg C/m^2) agree reasonably with observations for late summer (571 mg C/m^2; Roman et al., 1993). Model zooplankton concentrations in Slope water are 2–3 times higher than in the Sargasso, also in agreement with the observations (Ashjian et al., 1994).

3.1.6. New production, primary production and f-ratio

Vertically integrated new production (Fig. 4e) is high along most of the front, except between ($i = 35, j = 38$) and ($i = 42, j = 25$) where major downwelling occurs. Highest values are generally in or trailing downstream of upwelling zones, although agreement is not perfect. Consequently new production at the front is generally anti-correlated with the vertically integrated phytoplankton patches (Fig. 4c), which are due to downwelling. Upwelling on the Slope side of the front is more effective at enhancing new production than upwelling on the Sargasso side. The *f*-ratio (Fig. 4g) reaches up to 0.6 at the Gulf Stream front.

Vertically integrated primary production (Fig. 4f) does not show enhancement at the Gulf Stream front. This is because new production generally occurs in upwelled water parcels rich in NO_3 but poor in phytoplankton and recycled production, and generally underneath phytoplankton-poor surface water (Fig. 4e versus Fig. 4b). Thus, while a rim of additional production is added

at the front by new production, the Gulf Stream front primarily appears as a transition zone between the Sargasso and Slope waters, rather than as a local productivity maximum.

Our simulation agrees with the BIOSYNOP data that the cross-stream gradient in primary production is greater than the meander-related enhancement. In the Sargasso, our primary production estimate (170 mg $C/m^2/d$) is lower than observed during BIOSYNOP near the Gulf Stream (approx. 350 mg $C/m^2/d$; Lohrenz et al., 1993) but similar to values near Bermuda in August (96–261 mg $C/m^2/d$, Malone et al., 1993) to which the Sargasso was tuned. In Slope water, observed primary production during BIOSYNOP was approx. 450 mg $C/m^2/d$ downstream of the crest at ($i = 37$, $j = 35$), 550 mg $C/m^2/d$ in Slope water in general, and up to 700 mg $C/m^2/d$ upstream of the crest at ($i = 28$, $j = 39$), due to upwelling bringing the Chl maximum and nitricline into higher light levels (Lohrenz et al., 1993). In Run 6, primary production downstream of the crest and in Slope water in general agrees well with the data, but upstream and at the crest apex is lower than observed. This is because in the model the upwelling at ($i = 28$, $j = 38$) occurs primarily south of the front rather than north, which dilutes the phytoplankton (Fig. 4c) without adding significant nutrients. This illustrates the importance of the cross-stream position of the upwelling. Upwelling during BIOSYNOP was observed north of the front, more like that located at ($i = 22$, $j = 37$), which does locally enhance primary production values. Nevertheless, while Run 6 underestimates the primary production rate upstream of the crest, the simulated plankton distributions agree with the data, because the plankton spend less than half a day in the 40 km upwelling zone where growth rates are high, i.e. the high production rates are not observed to increase their biomass (Lohrenz et al., 1993).

3.1.7. Sinking particle export

The fast-sinking particle flux at 156 m (Fig. 4h) is similar to the zooplankton distribution, i.e. having slight enhancement at the Gulf Stream front. This is expected because the particle flux is parameterized as a function of zooplankton and phytoplankton concentration.

Our sinking detritus flux estimate in the Sargasso (1.7 mg $N/m^2/d$ at 150 m) agrees with summertime BATS data (1–5 mg $N/m^2/d$; http://www.bbsr.edu/users/ctd/). Unfortunately there is little particle flux data in Slope waters for comparison. If we assume that particle flux is proportional to primary production (Suess, 1980; Michaels et al., 1994), the summertime particle flux should be near 2–10 mg $N/m^2/d$ in Slope waters; our model value of 11 mg $N/m^2/d$ is therefore likely an overestimate. As we may be underestimating primary production in the Sargasso by a factor of 2 but get export correct, and get production correct in the Slope but may overestimate export by a factor of 2, this suggests we are putting too great a fraction of productivity into fast-sinking particles, and should be using a maximum fraction of 25% (Wefer, 1993) instead of 50% (Eppley and Peterson, 1979). This correction will be used in future work; it should cause little qualitative change in the results presented here, and should not alter our basic conclusions, because export at this time is a small fraction of production (1 mg $N/m^2/d = 5.7$ mg $C/m^2/d$).

An interesting aspect of the simulation is that particle export is often low where new production is high (Fig. 4h versus Fig. 4e), contrary to the formulation of most simple nutrient cycle models (Najjar et al., 1992; Anderson and Sarmiento, 1995). That is, the simulation suggests a significant temporal and spatial lag between the two in areas of high horizontal velocity. This result hinges on the parameterization that particle flux is a function of plankton biomass rather than new production. Phytoplankton biomass can lag new production when all the nitrate has not been

converted into biomass yet. Any lag between Z and P would contribute, and if F were modeled explicitly with a finite sinking speed, the lag would be increased further. This raises the issue of whether particle flux should be parameterized as a function of biomass, new production or primary production. A difficulty with having export depend on new or primary production is that these are zero at night; daily-averaged production values could be used, though this would also introduce a time lag. Correlation between primary production and particle export is not always observed (Michaels and Knap, 1996; Buesseler, 1998). Dependency on plankton biomass is not entirely correct either, because species size class is important; diatoms sink faster than picoplankton, and copepods form faster-sinking fecal pellets than protozoa. If large phytoplankton and zooplankton species control the particle flux, the question is whether their abundances are best expressed as functions of biomass, new production or primary production. Exploring this issue will require further data analysis and parameterization testing. Until then, the question remains regarding the appropriate temporal and spatial lags of particle export behind new production, primary production, and biomass. If seasonal storage into DOM is significant (Carlson et al., 1994; Doney et al., 1996), these lags could be quite large.

3.1.8. Summary of Run 6 results

Run 6 shows general agreement with the data. Contrary to original expectations, phytoplankton patches were not found to be correlated with or downstream of upwelling zones in the Gulf Stream. Patches at the sea surface were principally due to lateral detrainment of upwelled water away from the Gulf Stream; patches in vertically integrated plankton along the Stream were due to horizontal convergence and downwelling, i.e. physical processes rather than biological processes.

3.2. Run 7: the effect of winds

Run 7 was conducted to explore the effect of realistic wind forcing. In particular it was of interest to find out whether vertical velocities generated by winds override those due to meandering and ring–stream interactions at the base of the euphotic zone. Run 7 begins on 28 Sept. and is run for 10 d, identical to Run 6. ECMWF winds with 2.5° horizontal resolution and 12-hour temporal resolution for Sept.–Oct. 1988 are used to force the model. The winds have significant temporal variability in both magnitude and direction (Fig. 6). The mean wind stress during the simulation was 0.10 N/m^2 (corresponding wind speed: 7.5 m/s), with maximum values of 0.67 N/m^2 (wind speed: 19 m/s). A mixed-layer scheme (Anderson et al., 2000, Appendix A.1) is used which allows spatial and temporal mixed-layer depth variability as a function of wind speed and stratification. Comparison between Runs 6 and 7 will indicate the role of the wind at the Gulf Stream front. As Run 7 includes winds, it is our best reconstruction of the events that occurred during BIOSYNOP.

The winds appear to have little effect on the temperature evolution of the Gulf Stream (Fig. 7a–d; compare with Fig. 1), except for slightly cooler Slope water on day 10 related to mixed layer deepening. Vertical velocity at 42 m is also basically similar (Fig. 7e–h versus Fig. 3). The upwelling and downwelling caused by the meanders and ring–stream interactions are still present, and primarily have not been overridden by the winds. In Run 7 there is additional upwelling and downwelling at the stream axis and at rings caused by the winds (e.g. on day 10 at $i = 15$, $j = 31$). These wind-driven vertical velocities are short-lived and generally smaller than those caused by the meanders and ring–stream interactions.

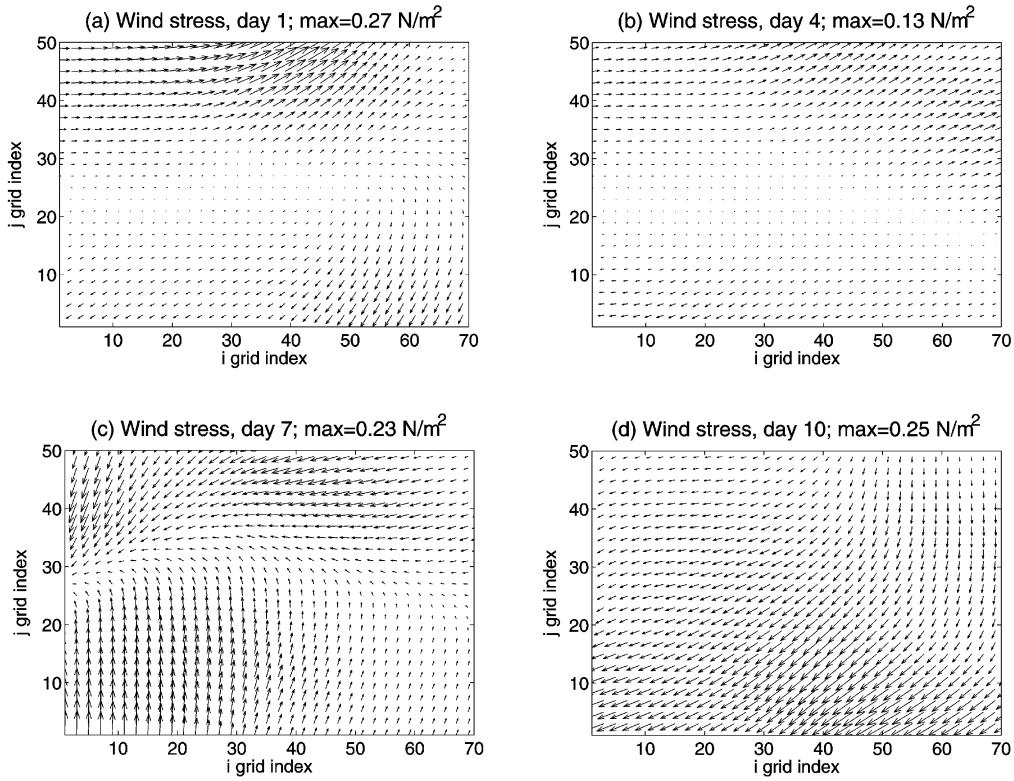

Fig. 6 . A subsample of the 12-hourly ECMWF surface winds used to force Run 7.

The winds cause significant horizontal surface velocities in the Slope and Sargasso surface waters (Fig. 8a–d; compare with Fig. 2). At times flows are generated perpendicular to the Gulf Stream front (e.g. on day 10), which temporarily displace the front. Because of the high temporal variability of the winds, these cross-frontal flows and displacements are short lived (approx. 1 day), often alternate in direction, and typically do not penetrate deeper than the mixed layer. Consequently there is little impact on the physical evolution of stream position, and, as the physical and biological fronts are displaced together, little impact on the cross-frontal flux of biological quantities. The integrated 10-day meridional advective flux of NO_3 in the top 100 m is only 1% higher in Run 7 than in Run 6, in part because surface NO_3 is very low. The meridional advective (southward) flux of phytoplankton in the top six meters (level 1) in Run 7 is twice that of Run 6, but the vertically integrated flux is only 6% higher. Thus, during this period, the winds have little effect on the temporally integrated meridional transport of biological tracers. It remains possible however that wind-driven cross-frontal advection is important on other time scales, during periods of persisted winds, or for wind events stronger than those that occurred during this period. It is also possible that in nature these small perturbations by winds contribute to the shedding of surface streamers on a scale that is not adequately resolved by the model's 15 km horizontal resolution; this would need to be examined in higher resolution simulations.

The spatial scale of the winds is too large and the temporal scale too short for the winds to directly generate mesoscale eddies in the Slope or Sargasso waters (Fig. 8), although the low

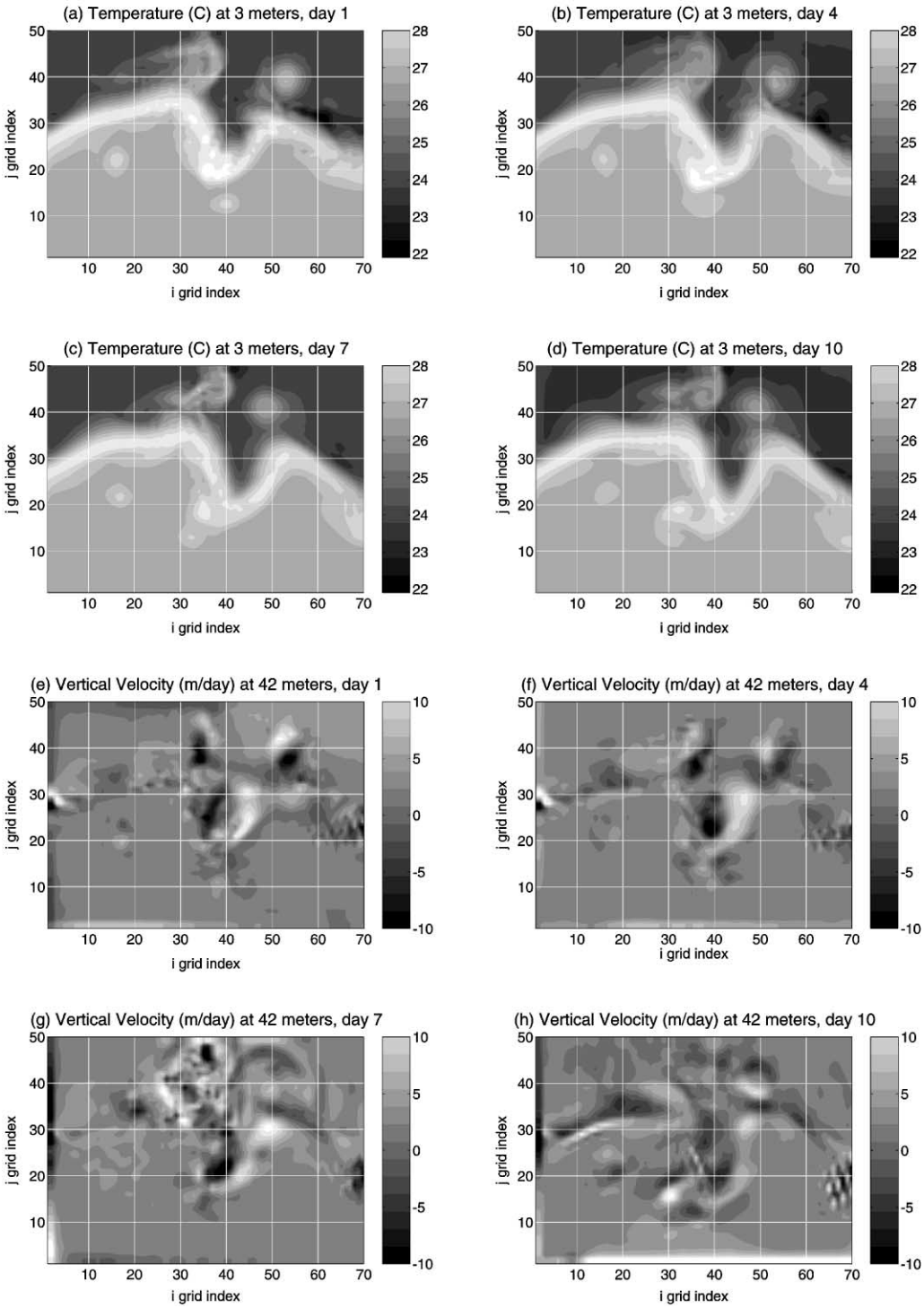

Fig. 7. Temperature and vertical velocity in Run 7.

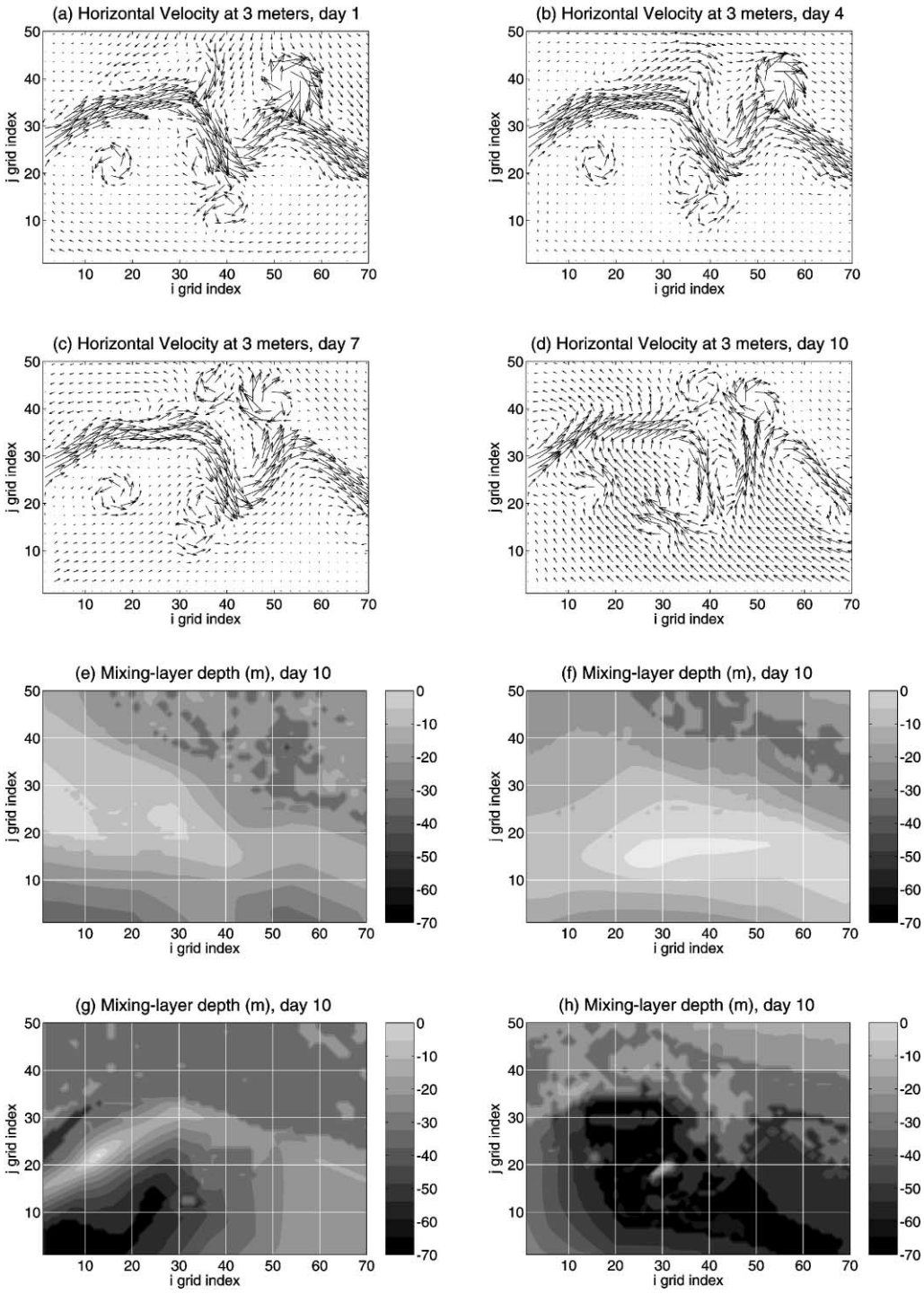

Fig. 8. Horizontal velocity and mixing-layer depth in Run 7. Mixing-layer depth is defined as the depth to which a vertical diffusivity of 50 cm^2/s is applied based on the wind stress and stratification, and may differ from the instantaneous and "target" mixed-layer depths (see Anderson et al., 2000).

frequency variations may contribute (Phillips, 1966; but see Pares-Sierra et al., 1993; Lippert and Müller, 1995). Therefore, in the 10-day simulation the winds do not generate mesoscale vertical velocities in the open ocean except near existing fronts or eddies.

Mixed layer depth (Fig. 8e–h) essentially varies proportionally to wind speed, shallowing when winds are weak (up to 10 m), and deepening where and when winds are strong (e.g. to 70 m on day 10). As the upper 80 m of the Sargasso are less stratified than in the Slope, mixed layer depths are generally deeper in the Sargasso than the Slope for a given wind speed. Consequently, the Gulf Stream front often appears as a boundary between regions of differing mixed layer depth (e.g. days 4 and 7).

Surface NO_3 concentrations (Fig. 9a) are increased by an order of magnitude in Slope waters when strong winds occur (compare Figs. 9a and 4a), due to mixed layer deepening and entrainment of nitrate from below; however values are still small (<0.1 μM) and surface Slope waters essentially nutrient depleted. Such nutrient entrainment does not occur in the Sargasso due to the great depth of the nutricline (80 m), although this might happen for stronger wind events than occur here, or in places of lifted isopycnals if mesoscale eddies were present in Sargasso waters.

Phytoplankton biomass (Fig. 9b and c) is slightly enhanced in Slope regions associated with higher mixed-layer nitrate (compare with Fig. 4), but the winds have not caused noticeable enhancement in biomass at the Gulf Stream front. Zooplankton concentrations (Fig. 9d) are slightly higher than in Run 6.

New production, primary production and particle flux (Fig. 9e–h) are all slightly higher in Slope waters than in Run 6 (Fig. 4) due to mixed layer deepening. The 10-day integrated primary production and particle flux at 156 m are only 2% higher in Run 7 than in Run 6, and new production is 1% higher. No enhancement is seen at the front itself. When the winds displace the position of the Gulf Stream front northward, the vertical shear of horizontal velocity at the base of the mixed layer is increased; even so, the mixed layer does not become deeper at the front than in neighboring water (Fig. 8e–h), and the vertical diffusive flux of NO_3 is not significantly enhanced at the front over that in Slope water. Thus wind-driven vertical velocities, vertical shear and cross-frontal transport appear to have little impact on production or particle flux at this time of year.

It was also investigated whether the data assimilation in Run 7 was inhibiting the impact of the winds. Simulations without data assimilation were therefore performed with and without winds. Again, while the winds significantly increased variability in the system, there was little net impact: vertically integrated primary production increased by 3%, new production by 9%, and particle flux at 156 m by 2% due to winds. The meridional advective flux of NO_3 (southward) in the upper 100 m was increased by 2%, and the meridional advective flux of phytoplankton (southward) by 11%. Furthermore, simulations without data assimilation and without rings (see Run 8), conducted with and without winds, confirmed that the winds during BIOSYNOP caused neglible enhancement in phytoplankton and new production at the front itself, and therefore are not the likely cause of the observed phytoplankton patch there.

In conclusion, while typical winds increase the spatial and temporal variability in the fields, and can generate significant horizontal and vertical velocities at the Gulf Stream front, these are generally short-lived events with minor temporally averaged effects. The winds generally do not override the internal dynamical vertical velocities at 42 m due to stream meandering and ring–stream interactions, and do not greatly enhance plankton biomass, production or particle flux

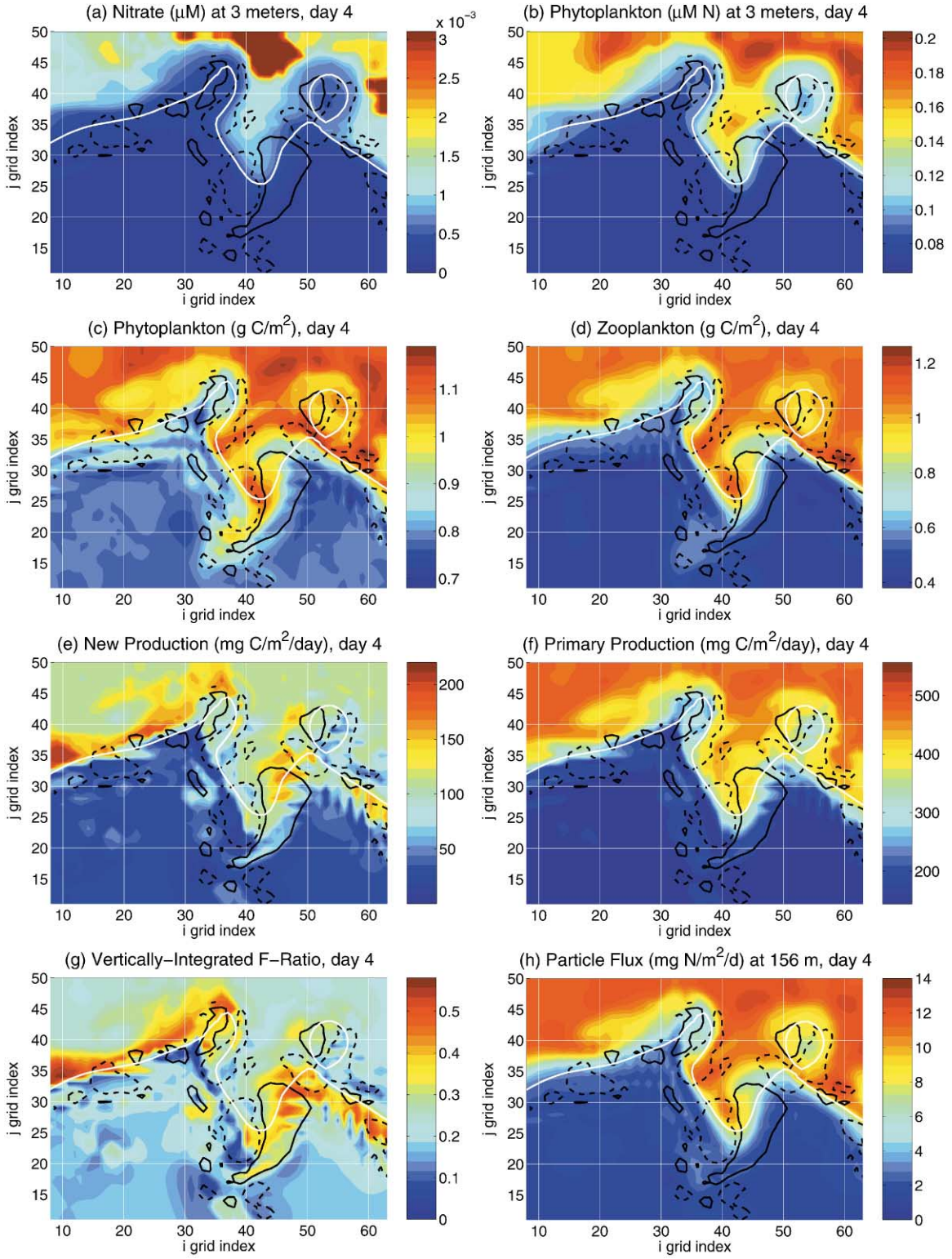
(a) Nitrate (μM) at 3 meters, day 4
x 10^-3
(b) Phytoplankton (μM N) at 3 meters, day 4
(c) Phytoplankton (g C/m^2), day 4
(d) Zooplankton (g C/m^2), day 4
(e) New Production (mg C/m^2/day), day 4
(f) Primary Production (mg C/m^2/day), day 4
(g) Vertically–Integrated F–Ratio, day 4
(h) Particle Flux (mg N/m^2/d) at 156 m, day 4
i grid index
j grid index

at the Gulf Stream front. However the wind speed does have an important influence on mixed layer depth and entrainment of nutrients from below in Slope waters.

3.3. Run 8: the effect of ring–stream interactions

The primary features of interest in Runs 1 through 7 are the enhanced nitrate and phytoplankton patches that occur at the sea surface in the central trough (Fig. 4a and b), and the vertically integrated phytoplankton and zooplankton patches east of the meander crest (Fig. 4c and d at $i = 36$, $j = 34$) which agree with the BIOSYNOP data. These are not due to the assimilation of BIOSYNOP data because the patches also occur in Run 2 (Fig. 10), which does not include any data assimilation. A remaining question was whether the convergence and divergence zones, and thus the patches, were primarily due to the stream meandering or due to the nearby ring–stream interactions. Run 8 was therefore conducted, identical to Run 2 but without the ring structures, in order to investigate the impact of stream meandering versus ring–stream interactions on the biological distributions.

3.3.1. Run 8 results

Run 8 shows the expected pattern of upwelling and downwelling associated with meanders (Fig. 11b). Comparison with Run 2 (Fig. 10b) shows that the rings intensified some of the vertical velocities and introduced additional zones. In particular the strong downwelling downstream of the meander crest (at $i = 37$, $j = 37$ in Fig. 10b), observed during BIOSYNOP, appears to be primarily due to the ring–stream interaction rather than the stream meandering. This is consistent with Hummon and Rossby (1998), who found this particular ring–stream interaction to intensify the trough downstream and to enhance the cross-stream exchange of water.

Without rings, surface nitrate and phytoplankton are no longer enhanced in the central trough (Fig. 11c and d; compare with Fig. 10), despite similarly high meander vertical velocities. This suggests that little water is detrained from the Gulf Stream by the meandering process alone. Rings impinging on the Gulf Stream, however, can pull off streamers, taking water laterally out of the Gulf Stream roller coaster, enhancing the net horizontal and vertical transport of nutrients and plankton. The net vertical advective flux of NO_3 is approximately 30% higher in Run 2 than in Run 8. The net meridional advective flux (southward) is 30% higher for NO_3 and 10% higher for phytoplankton. Diffusive fluxes in Run 8 and Run 2 are approximately the same, and no biological enhancement is seen in Run 8 due to detrainment of water from the Gulf Stream by horizontal diffusion. Thus the ring–stream interactions significantly enhance the net vertical transport and the cross-frontal exchange of biological quantities, through horizontal and vertical advection.

Vertically integrated phytoplankton in Run 8 (Fig. 11e) is slightly enhanced at the most intense part of the trough ($i = 43$, $j = 22$), but much less than in Run 2 (Fig. 10e). Negligible enhancement

Fig. 9. Biological fields on day 4 of Run 7. Vertical integration is over the upper 278 m, although plankton concentrations and production are generally negligible below 150 m. A C/N ratio of 6.625 mol/mol was used to convert from N to C (Redfield et al., 1963). The white contour is the location of the 15 C isotherm at 200 m, which approximates the location of the North Wall separating Gulf Stream and Slope waters. Solid (dashed) black contours indicate where upward (downward) vertical velocity at 42 m exceeds 2 m/d.

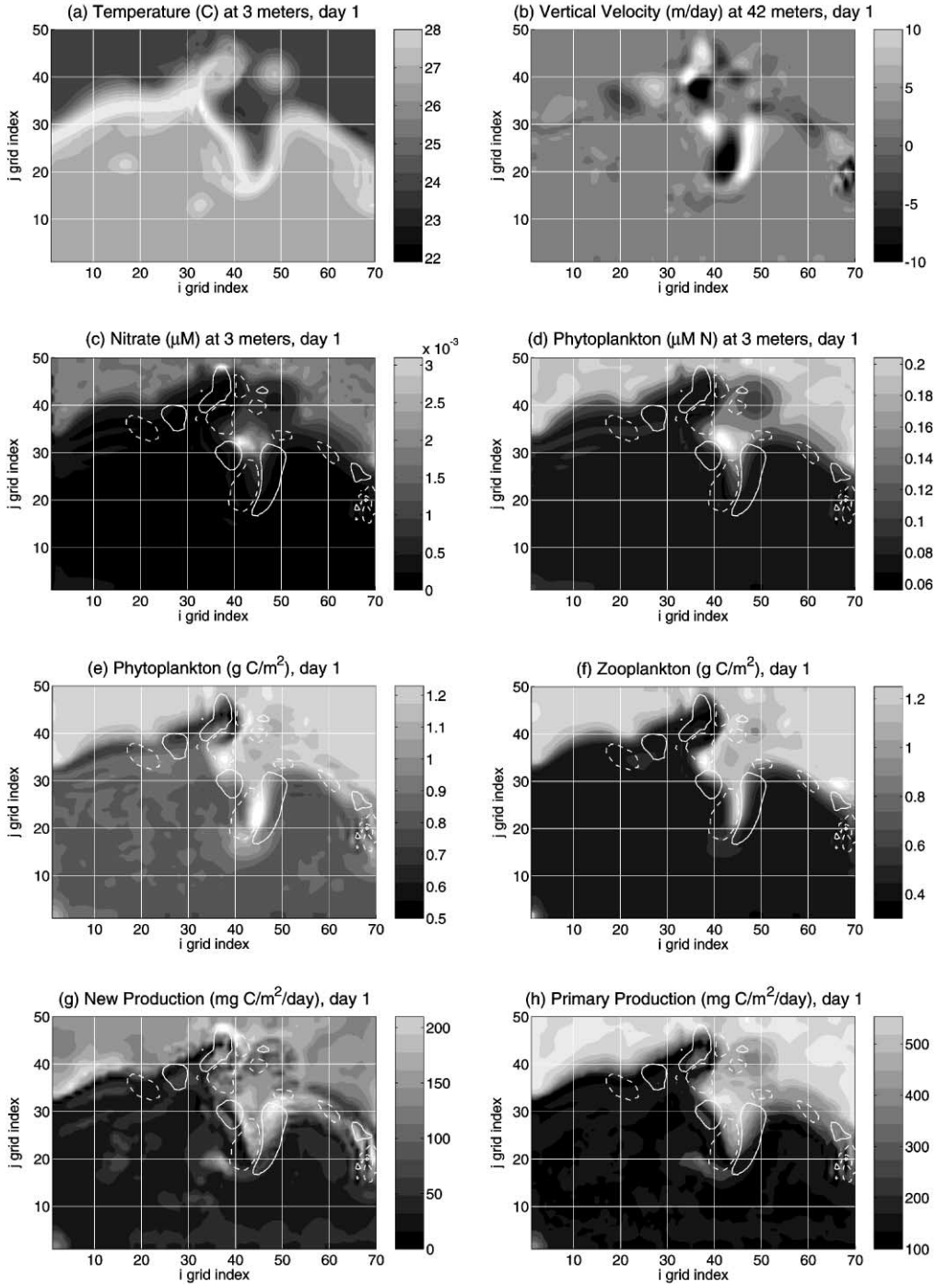

Fig. 10. Fields on day 1 of Run 2. Vertical integration is over the upper 278 m, although plankton concentrations and production are generally negligible below 150 m. A C/N ratio of 6.625 mol/mol was used to convert from N to C (Redfield et al., 1963). Solid (dashed) white contours indicate where upward (downward) vertical velocity at 42 m exceeds 3 m/d.

in vertically integrated zooplankton occurs at the front (Fig. 11f). The conclusion is that the ring–stream interactions rather than the meandering is the main cause of the phytoplankton and zooplankton patches at ($i = 38$, $j = 35$) in Fig. 10e and f observed during BIOSYNOP. Due to the almost continuous presence of warm core rings to the north of the Gulf Stream, often interacting with meander crests, ring–stream interactions may be the dominant local mechanism for creating plankton patches at the Gulf Stream front.

Run 8 suggests that, in the absence of ring–stream interactions, little enhancement occurs at the front. This agrees well with much of the ocean color data (e.g. CZCS at http://daac.gsfc.nasa.gov/) and in situ data (e.g. Hitchcock, 1988), which often do not detect enhancement at the front. That is, the hypothesis that meandering alone generally causes enhancement at the front and in trough recirculations (e.g. Olson et al., 1994) does not agree with much of the data. The fact that enhancement is only sometimes observed (Section 1) indicates that only the most intense phenomena, such as ring–stream interactions, cause enhancement.

The fact that ring–stream interactions are the main cause of patchiness in our simulations, stresses the importance of resolving not just the mesoscale features but the submesoscale interaction zones and events (e.g. Dutkiewicz and Paldor, 1994) for accurately simulating nutrient transports and plankton distributions. Although we used as high a grid resolution as we could at the time, 15 km resolution resolves these interaction zones coarsely, and it is desirable to test the sensitivity of the results to grid resolution. Higher horizontal resolution may allow stronger gradients and higher vertical velocities, as have been observed on occasion (e.g. up to 4–6 mm/s = 350–520 m/d; Lindstrom et al., 1997; Hummon et al., 1991). Nevertheless, as our grid resolution is a fraction of the Rossby radius, we should not be missing the basic processes; this is supported by the fact that the data are reasonably explained by our simulations.

3.3.2. New production at the Gulf Stream front

Gulf Stream meandering *does* enhance new production (= vertical NO_3 transport) at the front (Fig. 11g). However, this new production does not enhance vertically integrated phytoplankton or primary production at the front over that of Slope water (Fig. 11e and h; also Section 3.1.6). The enhancement at the front is "hidden" because production and plankton are relatively high in Slope waters, due to the nutricline being at the base of the mixed layer. If the waters to the north were more oligotrophic, the effect of the meadering would be more apparent (e.g. Dadou et al., 1996).

New production at the front reaches up to 0.26 g $C/m^2/d$ in Run 2. This is on the low end of estimates for mesoscale eddies in the Sargasso based on models of similar resolution; McGillicuddy and Robinson (1997, Fig. 10) estimate new production to frequently get up to 1–3 mol $N/m^2/yr = 0.22$–0.65 g $C/m^2/d$, and Mahadevan and Archer (2000; their 0.2° simulation) get values up to 40 mol $C/m^2/yr = 1.3$ g $C/m^2/d$. Why isn't new production at the Gulf Stream front higher?

The first point to note is that, in meander troughs, downwelling precedes upwelling, which should decrease rather than increase productivity. Indeed, vertically integrated phytoplankton is enhanced at the southern tip of the trough (Fig. 11e) only due to convergence. Enhancement could occur downstream of troughs if the downwelling led to a net transfer of NO_3 across isopycnals, but this does not occur in our simulations. Enhanced new production is only expected upstream of meander crests, and this is where it is primarily found (Fig. 11g).

In Run 8, the NO_3 distribution agrees well with the data, and the vertical velocities at 68 m are even larger than in McGillicuddy and Robinson (1997) (who reported several m/d). In fact, the

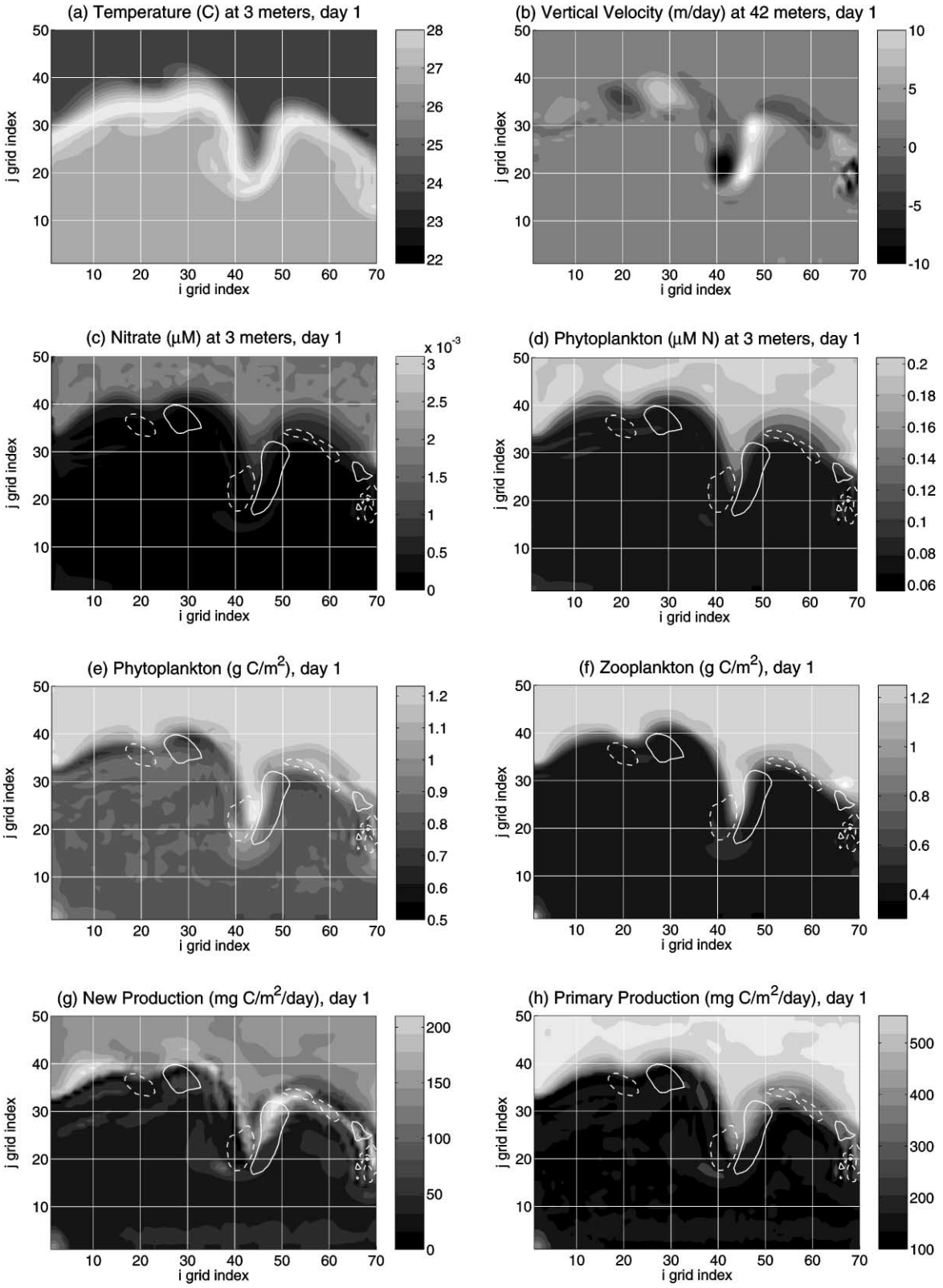
(a) Temperature (C) at 3 meters, day 1
(b) Vertical Velocity (m/day) at 42 meters, day 1
(c) Nitrate (μM) at 3 meters, day 1
x 10^-3
(d) Phytoplankton (μM N) at 3 meters, day 1
(e) Phytoplankton (g C/m^2), day 1
(f) Zooplankton (g C/m^2), day 1
(g) New Production (mg C/m^2/day), day 1
(h) Primary Production (mg C/m^2/day), day 1
j grid index
i grid index

maximum NO_3 flux at 68 m in Run 8 on day 1 (which occurs at $i = 47, j = 31$) is 21 mmol N/m^2/d = 7.7 mol N/m^2/yr, higher than most NO_3 fluxes that occur in McGillicuddy and Robinson (1997) and Mahadevan and Archer (2000). Highest new production rates occur just below the mixed layer (on levels 6 and 7, 32–54 m) at the Chl maximum at the top of the Slope water nutricline. In Run 8 on day 1 on level 6, the new production rate at ($i = 47, j = 31$) is 0.09 mmol N/m^3/d. There is significant NH_4 at and below the Chl maximum, such that the *f*-ratio is 0.64. The phytoplankton concentration is 0.21 μM N, and their doubling timescale is 1.4 d; this is the maximum for this light intensity, i.e. the phytoplankton are not nutrient limited. Even though phytoplankton in the Chl maximum increase downstream of the upwelling zone (by approximately 50%), not all the NO_3 is taken up; the size of the upwelling and downwelling zones is typically 150 km or less (Fig. 11b), such that phytoplankton at the front traveling at 1.5 m/s (=130 km/d) are swept through these zones in a day or less. Consequently only about 0.1 μM of NO_3 is consumed, and a significant amount of NO_3 is brought back down. The NO_3 uptake rate would be higher if phytoplankton biomass were higher, but biomass is limited because, after a single day of net growth, they are sent back down to the depths for decimation. As our biological model assumes instantaneous photoadaptation, the actual enhancement by Gulf Stream meanders should be even less.

This illustrates a significant difference between physical–biological coupling in the Gulf Stream and in mid-ocean eddies. At the Gulf Stream front, the timescale of physical events in the Lagrangian frame (approx. 1 d) is shorter than the biological doubling timescale (a few days), resulting in a rather small biological response (Olson et al., 1994). In the open ocean, horizontal velocities are lower, such that physical timescales (several days) are often longer than biological timescales, which should allow larger biological responses. The greatest biological response should be caused by vertical excursions that last a week or more, which would allow the phytoplankton to adjust to their new light regime and utilize the nutrients before being returned to depth. Assuming an upwelling zone 100 km in length, a 1-week timescale corresponds with a horizontal velocity of 17 cm/s — a moderate ocean eddy. Recent observations and modeling studies support the importance of such common mesoscale features (Strass, 1992; Dadou et al., 1996; McGillicuddy and Robinson, 1997). Other studies (Fasham et al., 1985; Falkowski et al., 1991), however, report little observed biological enhancement due to moderate mesoscale features. Apparently the degree of biological enhancement depends strongly on the variable relationship between the magnitude and Lagrangian duration of the isopycnal displacements and the Chl, NO_3 and light distributions. Dadou et al. (1996) note the significant dependency of biological response to the upwelling duration of eddies. A general theory of the impact of advection on biological dynamics is given by Robinson (1997).

It remains possible that if our simulations were run for a longer period, higher new productivity events would occur (as in McGillicuddy and Robinson, 1997). However, the ring absorption event in our simulations is about as intense as events come. It is also possible new production would be higher in our simulations if higher grid resolution were used (Mahadevan and Archer, 2000).

Fig. 11. Fields on day 1 of Run 8. Vertical integration is over the upper 278 m, although plankton concentrations and production are generally negligible below 150 m. A C/N ratio of 6.625 mol/mol was used to convert from N to C (Redfield et al., 1963). Solid (dashed) white contours indicate where upward (downward) vertical velocity at 42 m exceeds 3 m/d.

However this still would not explain why our new production estimates are lower than Sargasso estimates, because similar resolution is used (McGillicuddy and Robinson use 15.6 km resolution; Mahadevan and Archer's 0.2°resolution = 18 km).

It is also possible that the McGillicuddy and Robinson (1997) and Mahadevan and Archer (2000) estimates are too high. McGillicuddy and Robinson (1997) use an uptake timescale of 15 min, which may overestimate new production. Mahadevan and Archer (2000) use a euphotic zone depth of 160 m, to offset the underestimate in their NO_3 profile; because vertical velocity magnitudes increase with depth, they may overestimate the NO_3 flux through the base of the euphotic zone. In any case, both physical and biological timescales associated with eddies can be in the vicinity of a few days, such that it is important to estimate each accurately. The actual NO_3 uptake rate varies with depth due to biomass concentration and light limitation, and may evolve in time in a complex manner due to changes in biomass and self-shading. The presence of NH_4 at the subsurface Chl maximum will reduce the NO_3 uptake rate. It will be important to verify the McGillicuddy and Robinson (1997) and Mahadevan and Archer (2000) results with more complex biological models, or at least test their sensitivity to the biological timescale and euphotic zone depth used.

Three other processes, not included in our simulations, also may contribute to phytoplankton patchiness along the Gulf Stream. The first is positive buoyancy or upward swimming of phytoplankton cells (Franks, 1992), which would enhance their tendency to collect in downwelling zones as observed. Because the phytoplankton pass through the downwelling zones in about 1 d, this upward motion would need to be on the order of 10 m/d to have an observable impact. Such behavior for phytoplankton in the Gulf Stream remains to be demonstrated. A second, related process would be zooplankton vertical migration inducing phytoplankton variability through predator–prey interactions. However, because the observations show the zooplankton patch is spatially correlated with the phytoplankton patch, grazing is not a likely mechanism for explaining the BIOSYNOP phytoplankton distribution. The third process is entrainment of continental shelf water at Cape Hatteras (Lillibridge et al., 1990), which may be a source of biomass directly or through the recycling of other organic nitrogen forms (Olson et al., 1994). Shelf water entrainment is apparent in some of the CZCS images; therefore this process cannot be ruled out as contributing to the patchiness observed during BIOSYNOP. However our simulations reproduce the patches observed during BIOSYNOP without resorting to this process.

4. Discussion: Comparison with previous studies

Previous modeling studies of physical–biological processes at fronts have been rather disparate, in their focus and their conclusions. Here we thought a general discussion would be useful, to synthesize our findings with previous work, to arrive at a better picture of the dominant physical–biological interactions at the Gulf Stream front in summer.

Flierl and Davis (1993) examined physical–biological interactions in a meandering jet with a two-layer quasigeostrophic model and a P-N-Z biological model. Their results and ours are similar in several respects. They computed similar patterns and magnitudes of vertical velocities associated with meanders as we have. Their model shows enhanced phytoplankton values associated with ring formation, similar to our ring–stream interaction. Their phytoplankton enhancement due to meandering (10–20%) is small relative to the cross-frontal gradient in phytoplankton.

They obtain high phytoplankton concentrations downstream of crests, as we do and as observed in BIOSYNOP. However in their model this is due to phytoplankton growth in response to increased nutrients (upwelled upstream of the crest), whereas in our model it is due to horizontal convergence. Thus while the distributions agree, the dynamics that create the distributions differ. They obtain high zooplankton concentrations downstream of troughs, due to zooplankton growth in response to increased phytoplankton. This disagrees with the BIOSYNOP data, which show the zooplankton maximum downstream of the crest (Olson et al., 1994), and too close behind the phytoplankton patch to be due to growth (Ashjian et al., 1994).

Actually our simulations do have dynamics similar to Flierl and Davis (1993) at the subsurface Chl maximum (levels 6–8, 32–68 m), where upwelling upstream of meander crests causes new production and phytoplankton maxima near the apex of the crests, followed by zooplankton maxima a short distance downstream, approximately in the downwelling zones. The important differences with Flierl and Davis (1993) however are that (a) this only occurs on levels 6–8; it does not appear in the vertical integrals nor in the sea surface (mixed layer) concentrations; and (b) the spatial lags are relatively short, such that zooplankton and phytoplankton are more correlated than anticorrelated.

Flierl and Davis (1993) get a spatial anti-correlation between phytoplankton zooplankton probably in part due to their low vertical resolution (2 levels). Upwelling increases nutrients but dilutes plankton in the mixed layer, which initiates a phytoplankton bloom followed by a zooplankton bloom; these are separated in space due to horizontal advection. In our simulations, where the higher vertical resolution allows subsurface plankton maxima at the top of the nitricline, upwelling increases nutrients, phytoplankton and zooplankton in the mixed layer, in agreement with the data (see cross sections in Lohrenz et al., 1993; Hitchcock et al., 1993). Consequently, the ecosystem is less out of balance, and any bloom response is much reduced. Secondly, the phytoplankton and zooplankton patches are primarily created by horizontal convergence, causing spatial correlation rather than anti-correlation. Their physical model cannot accurately take into account this horizontal convergence. Finally, the fact that their biological model's steady-state solution is discontinuous with depth may contribute to an oscillatory response to upwelling. Nevertheless, while their dynamics do not adequately explain the BIOSYNOP data, it is possible such predator–prey oscillations cause patchiness at other fronts, or at the Gulf Stream at other times or locations.

Olson et al. (1994) conducted a simulation of a Gulf Stream meander using a three-layer isopycnic model and a N-P-Z-D biological model. They obtain high phytoplankton concentrations following the meander crest, described as due to advection and diffusion concentrating phytoplankton in the meander trough recirculation, and suggest that the horizontal advection of phytoplankton through meanders is too fast for the phytoplankton to respond to increased light levels, as we find. However, they obtain zooplankton concentrations anti-correlated with phytoplankton, which is not consistent with the observations. This anticorrelation suggests control of Z in their model by biological processes (i.e. predator–prey oscillations) rather than physical processes (i.e. convergence, which would cause correlation). As their model is not described in detail, it is difficult to know why this happens; possibly for reasons similar to Flierl and Davis (1993). Their discussion of physical–biological processes at fronts is excellent.

Dadou et al. (1996) examined the effect of the meandering of the North Equatorial Current using a two-layer quasigeostrophic model and N–P–Z/N–P–Z–D biological models. Although not

strictly comparable to the Gulf Stream, they found that the jet meandering enhanced phytoplankton biomass up to 26%, which is greater than the enhancement found for the Gulf Stream by Flierl and Davis (1993) using a similar model. This is most likely due to the fact that their jet (10 cm/s) is weaker than the Gulf Stream, the more slowly evolving eddy motion causing a more significant biological impact (Section 3.3.2). They also get decoupling between new production and particle export as we do.

Franks and Walstad (1997) examined the effect of wind bursts on vertical velocity and phytoplankton enhancement at an idealized open ocean front using a two-dimensional (y–z) physical model and a N–P–Z biological model. Their findings are generally similar to ours, with minor enhancement in phytoplankton due to winds, except as a result of entrainment from mixed layer deepening. They obtained oscillations in vertical velocity at the Coriolis frequency following wind forcing. We found similar oscillations in preliminary simulations using constant wind forcing; however, with ECMWF wind forcing, these oscillations generally did not happen, because the ever-changing winds prescribe new horizontal and vertical velocities each day. Our simulations also indicate that the effect of winds on vertical velocities at the Gulf Stream front are generally minor compared to those due to jet meandering, except possibly in cases of very strong or persisted winds (Xue and Bane, 1997; Lee et al., 1994). In three dimensions, persisted wind stress curl can cause surface divergence and upwelling, as occurs in the equatorial regions and the Southern Ocean, which can have a significant impact on biological concentrations and processes (Lutjeharms et al., 1985).

5. Summary of conclusions

The following conclusions apply to summer conditions.

(1) Vertical velocities associated with Gulf Stream meanders do enhance new production at the front. However because phytoplankton are advected through the upwelling zones fairly quickly with respect to their doubling timescales, and because the new production generally occurs in water parcels poor in recycled production and phytoplankton, the meadering process does not enhance phytoplankton biomass, primary production or particle flux over that of Slope water. Consequently, meandering does not appear to be the primary cause of phytoplankton maxima found at the front. This is consistent with the fact that most often little to no enhancement in phytoplankton and primary production is observed at the Gulf Stream front.

(2) Ring–stream interactions are an important process for generating phytoplankton patches at the Gulf Stream front. Ring–stream interaction events cause high vertical velocities, which combine with horizontal velocities to laterally detrain upwelled or downwelled water from the Gulf Stream via streamers. This causes significant net vertical transports of nutrients and plankton, and consequently enhanced phytoplankton biomass either through advection or enhanced growth due to increased nutrients. Ring–stream interaction events also enhance meridional cross-frontal exchange. This emphasizes the importance of submesoscale interaction events in explaining the observed phytoplankton distributions at the Gulf Stream front.

Our simulations are in good agreement with the BIOSYNOP observations and with BATS data in the Sargasso. The high vertically integrated phytoplankton and zooplankton values found after

the meander crest during BIOSYNOP were most likely due to advection (convergence) intensified by the ring–stream interaction rather than biological growth in response to jet meandering as previously speculated. Surface phytoplankton patches that collect in meander trough recirculation gyres are most likely due to detrainment of nutrients and plankton from the Gulf Stream by ring–stream interactions.

(3) Winds affect biological tracers in two ways. The first is their influence on mixed-layer depth and the vertical entrainment/detrainment of nutrients and plankton. Significant responses due to these processes were found in Slope waters, because the nutricline and Chl maximum are at the base of the mixed layer. The second influence of winds is the driving of surface convergence or divergence and therefore vertical advection. It was found that although winds can generate upwelling and downwelling at the Gulf Stream front, they are generally short-lived and do not override the vertical velocities due to meandering. In addition while winds can drive large horizontal velocities, these generally do not extend below the mixed layer, and have little effect on the meridional transport of nutrients and plankton. Both of these are because of the high temporal variability in wind direction in mid-latitudes. Overall the simulations show no significant biological enhancement at the Gulf Stream front due to winds during this period.

(4) This study demonstrates that realistic high-resolution 4-D dynamical field estimates (simulations), brought into close correlation with observations by data assimilation, are generally necessary to identify the essential physical–biological interactions that explain the data.

Acknowledgements

We would like to thank (alphabetically) for data aquisition S. Fontana, J. Lillibridge, S. Lohrenz, A. Mariano, D. Olson, D. Phinney, T. Rossby, and G. Samuels; for modeling assistance A. Gangopadhyay, W. Leslie and C. Lozano; and J. McCarthy and three anonymous reviewers for helpful comments. The primary support for this work was provided by the UCAR Postdoctoral Program in Ocean Modeling and ONR grant N00014-95-1-0371 at Harvard. Additional support for completion of the manuscript was provided by NSF grant OCE-9725974 and ONR grant N00014-98-1-0608 to D. McGillicuddy at WHOI.

References

Anderson, L.A., Robinson, A.R., Lozano, C.J., 2000. Physical and biological modeling in the Gulf Stream region: I. Data assimilation methodology. Deep-Sea Research I 47, 1787–1827.

Anderson, L.A., Sarmiento, J.L., 1995. Global ocean phosphate and oxygen simulations. Global Biogeochemical Cycles 9, 621–636.

Ashjian, C.J., 1993. Trends in copepod species abundances across and along a Gulf Stream meander: evidence for entrainment and detrainment of fluid parcels from the Gulf Stream. Deep-Sea Research I 40, 461–482.

Ashjian, C.J., Smith, S.L., Flagg, C.N., Mariano, A.J., Behrens, W.J., Lane, P.V.Z., 1994. The influence of a Gulf Stream meander on the distribution of zooplankton biomass in the Slope Water, the Gulf Stream, and the Sargasso Sea, described using a shipboard acoustic Doppler current profiler. Deep-Sea Research I 41, 23–50.

Bleck, R., Onken, R., Woods, J.D., 1988. A two-dimensional model of mesoscale frontogenesis in the ocean. Quarterly Journal of the Royal Meteorological Society 114, 347–371.

Bower, A.S., 1991. A simple kinematic mechanism for mixing fluid parcels across a meandering jet. Journal of Physical Oceanography 21, 173–180.

Bower, A.S., Rossby, T., 1989. Evidence of cross-frontal exchange processes in the Gulf Stream based on isopycnal RAFOS float data. Journal of Physical Oceanography 19, 1177–1190.

Brzezinski, M.A., 1988. Vertical distribution of ammonium in stratified oligotrophic waters. Limnology and Oceanography 33, 1176–1182.

Buesseler, K.O., 1998. The decoupling of production and particle export in the surface ocean. Global Biogeochemical Cycles 12, 297–310.

Carlson, C.A., Ducklow, H.W., Michaels, A.F., 1994. Annual flux of dissolved organic carbon from the euphotic zone in the northwestern Sargasso Sea. Nature 371, 405–408.

Claustre, H., Kerhervé, P., Marty, J.C., Prieur, L., Videau, C., Hecq, J.-H., 1994. Phytoplankton dynamics associated with a geostrophic front: Ecological and biogeochemical implications. Journal of Marine Research 52, 711–742.

Dadou, I., Garçon, V., Andersen, V., Flierl, G.R., Davis, C.S., 1996. Impact of the North Equatorial Current meandering on a pelagic ecosystem: A modeling approach. Journal of Marine Research 54, 311–342.

Doney, S.C., Glover, D.M., Najjar, R.G., 1996. A new coupled, one-dimensional biological-physical model for the upper ocean: Applications to the JGOFS Bermuda Atlantic Time-series Study (BATS) site. Deep-Sea Research II 43, 591–624.

Dutkiewicz, S., Griffa, A., Olson, D.B., 1993. Particle diffusion in a meandering jet. Journal of Geophysical Research 98, 16,487–16,500.

Dutkiewicz, S., Paldor, N., 1994. On the mixing enhancement in a meandering jet due to the interaction with an eddy. Journal of Physical Oceanography 24, 2418–2423.

Eppley, R.W., Peterson, B.J., 1979. Particulate organic matter flux and planktonic new production in the deep ocean. Nature 282, 677–680.

Falkowski, P.G., Ziemann, D., Kolber, Z., Bienfang, P.K., 1991. Role of eddy pumping in enhancing primary production in the ocean. Nature 253, 55–58.

Fasham, M.J.R., Platt, T., Irwin, B., Jones, K., 1985. Factors affecting the spatial pattern of the deep chlorophyll maximum in the region of the Azores front. Progress in Oceanography 14, 129–165.

Flierl, G.R., Davis, C.S., 1993. Biological effects of Gulf Stream meandering. Journal of Marine Research 51, 529–560.

Franks, P.J.S., 1992. Sink or swim-accumulation of biomass at fronts. Marine Ecology Progress Series 82, 1–12.

Franks, P.J.S., Walstad, L.J., 1997. Phytoplankton patches at fronts: a model of formation and response to wind events. Journal of Marine Research 55, 1–29.

Furuya, K., 1990. Subsurface chlorophyll maximum in the tropical and subtropical western Pacific Ocean: vertical profiles of phytoplankton biomass and its relationship with chlorophyll *a* and particulate organic carbon. Marine Biology 107, 529–539.

Gould, R.W., Wiesenburg, D.A., 1990. Single-species dominance in a subsurface phytoplankton concentration at a Mediterranean Sea front. Limnology and Oceanography 35, 211–220.

Halkin, D., Rossby, H.T., 1985. The structure and transport of the Gulf Stream at 73 deg W. Journal of Physical Oceanography 15, 1439–1452.

Haney, J.D., Jackson, G.A., 1996. Modeling phytoplankton growth rates. Journal of Plankton Research 18, 63–85.

Heilmann, J.P., Richardson, K., Ærtejerg, G., 1994. Annual distribution and activity of phytoplankton in the Skagerrak/Kattegat frontal region. Marine Ecology Progress Series 112, 213–223.

Hitchcock, G.L., 1988. Plankton biomass and the physical field in fronts of oceanic current systems. In: Thompson, M.F., Tirmizi, N.M. (Eds.), Marine Science of the Arabian Sea. American Institute of Biological Sciences, Washington, DC, pp. 47–57.

Hitchcock, G.L., Mariano, A.J., Rossby, T., 1993. Mesoscale pigment fields in the Gulf Stream: observations in a meander crest and trough. Journal of Geophysical Research 98, 8425–8445.

Hummon, J.M., Rossby, T., 1998. Spatial and temporal evolution of a Gulf Stream crest-warm core ring interaction. Journal of Geophysical Research 103, 2795–2809.

Hummon, J., Rossby, T., Carter, E., Lillibridge, J., Liu, M., Schultz Tokos, K., Anderson-Fontana, S., Mariano, A., 1991. The Anatomy of Gulf Stream Meanders, Vols. 1 and 2. Technical Report 91-4. University of Rhode Island, 488pp.

Le Fèvre, J., Frontier, S., 1988. Influence of temporal characteristics of physical phenomena on plankton dynamics, as shown by North–West European marine ecosystems. In: Rothschild, B.J. (Ed.), Toward a Theory on Biological-Physical Interactions in the World Ocean. Kluwer Publishers, Dordrecht, pp. 245–272.

Lee, D.-K., Niiler, P., Warn-Varnas, A., Piacsek, S., 1994. Wind-driven secondary circulation in ocean mesoscale. Journal of Marine Research 52, 371–396.

Levine, E.R., Connors, D.N., Cornillon, P.C., Rossby, H.T., 1986. Gulf Stream kinematics along an isopycnal float trajectory. Journal of Physical Oceanography 16, 1317–1328.

Lillibridge, J.L., Hitchcock, G., Rossby, T., Lessard, E., Mork, M., Golmen, L., 1990. Entrainment and mixing of Shelf/Slope waters in the near-surface Gulf Stream. Journal of Geophysical Research 95, 13,065–13,087.

Lindstrom, S.S., Qian, X., Watts, D.R., 1997. Vertical motion in the Gulf Stream and its relation to meanders. Journal of Geophysical Research 102, 8485–8503.

Lindstrom, S.S., Watts, D.R., 1994. Vertical motion in the Gulf Stream near 68 deg W. Journal of Physical Oceanography 24, 2321–2333.

Lippert, A., Müller, P., 1995. Direct atmospheric forcing of geostrophic eddies. Part II: Coherence maps. Journal of Physical Oceanography 25, 106–121.

Liu, M., Rossby, T., 1993. Observations of the velocity and vorticity structure of Gulf Stream meanders. Journal of Physical Oceanography 23, 329–345.

Lohrenz, S.E., Cullen, J.J., Phinney, D.A., Olson, D.B., Yentsch, C.S., 1993. Distribution of pigments and primary production in a Gulf Stream meander. Journal of Geophysical Research 98, 14,545–14,560.

Longhurst, A.R., Harrison, W.G., 1989. The biological pump: Profiles of plankton production and consumption in the upper ocean. Progress in Oceanography 22, 47–123.

Lozano, C.J., Robinson, A.R., Arango, H.G., Gangopadhyay, A., Sloan, N.Q., Haley, P.J., Leslie, W.G., 1996. An interdisciplinary ocean prediction system: Assimilation strategies and structured data models. In: Malanotte-Rizzoli, P. (Ed.), Modern Approaches to Data Assimilation in Ocean Modeling, Elsevier Oceanography Series. Elsevier, Amsterdam, pp. 413–452.

Lutjeharms, J.R.E., Walters, N.M., Allanson, B.R., 1985. Oceanic frontal systems and biological enhancement. In: Siegfried, W.R., Condy, P.R., Laws, R.M. (Eds.), Antarctic Nutrient Cycles and Food Webs.. Springer, Berlin, pp. 11–21.

Mahadevan, A., Archer, D., 2000. Modeling the impact of fronts and mesoscale circulation on the nutrient supply and biogeochemistry of the upper ocean. Journal of Geophysical Research 105, 1209–1225.

Malone, T.C., Pike, S.E., Conley, D.J., 1993. Transient variations in phytoplankton productivity at the JGOFS time series station. Deep-Sea Research I 40, 903–924.

Mariano, A.J., Hitchcock, G.L., Ashjian, C.J., Olson, D.B., Rossby, T., Ryan, E., Smith, S.L., 1996. Principal component analysis of biological and physical variability in a Gulf Stream meander crest. Deep-Sea Research I 43, 1531–1565.

McGillicuddy, D.J., Robinson, A.R., 1997. Eddy-induced nutrient supply and new production in the Sargasso Sea. Deep-Sea Research I 44, 1427–1449.

Michaels, A.F., Knap, A.H., 1996. Overview of the U.S. JGOFS Bermuda Atlantic Time-series Study and the Hydrostation S program. Deep-Sea Research II 43, 157–198.

Michaels, A.F., Knap, A.H., Dow, R.L., Gundersen, K., Johnson, R.J., Sorensen, J., Close, A., Knauer, G.A., Lohrenz, S.E., Asper, V.A., Tuel, M., Bidigare, R., 1994. Seasonal patterns of ocean biogeochemistry at the U.S. JGOFS Bermuda Atlantic Time-series Study site. Deep-Sea Research I 41, 1013–1038.

Najjar, R.G., Sarmiento, J.L., Toggweiler, J.R., 1992. Downward transport and fate of organic matter in the ocean: Simulations with a general circulation model. Global Biogeochemical Cycles 6, 45–76.

Olson, D.B., Hitchcock, G.L., Mariano, A.J., Ashjian, C.J., Peng, G., Nero, R.W., Podesta, G.P., 1994. Life on the edge: Marine life and fronts. Oceanography 7 (2), 52–60.

Onken, R., 1992. Mesoscale upwelling and density finestructure in the seasonal thermocline — a dynamical model. Journal of Physical Oceanography 22, 1257–1273.

Osgood, K.E., Bane, J.M., 1987. Vertical velocities and dynamical balances in Gulf Stream meanders. Journal of Geophysical Research 92, 13,029–13,040.

Owen, R.W., 1981. Fronts and eddies in the sea: Mechanisms, interactions and biological effects.. In: Longhurst, A.R. (Ed.), Analysis of Marine Ecosystems.. Academic Press, London, pp. 197–233.

Pares-Sierra, A., White, W.B., Tai, C.-K., 1993. Wind-driven coastal generation of annual mesoscale eddy activity in the California current. Journal of Physical Oceanography 23, 1110–1121.

Pelegrí, J.L., Csanady, G.T., 1994. Diapycnal mixing in western boundary currents. Journal of Geophysical Research 99, 18,275–18,304.

Phillips, N.A., 1966. Large-scale eddy motion in the western Atlantic. Journal of Geophysical Research 71, 3883–3891.

Pollard, R.T., Regier, L.A., 1992. Vorticity and vertical circulation at an ocean front. Journal of Physical Oceanography 22, 609–625.

Prieur, L., Sournia, A., 1994. "Almofront-1" (April–May 1991): An interdisciplinary study of the Almeria-Oran geostrophic front, SW Mediterranean Sea. Journal of Marine Systems 5, 187–203.

Redfield, A.C., Ketchum, B.H., Richards, F.A., 1963. The influence of organisms on the composition of sea-water. In: Hill, M.N. (Ed.), The Sea. Vol. 2. Interscience, New York, pp. 26–77.

Robinson, A.R., 1997. On the theory of advective effects on biological dynamics in the sea. Proceedings of the Royal Society of London A 453, 2295–2324.

Roman, M.R., Dam, H.G., Gauzens, A.L., Napp, J.M., 1993. Zooplankton biomass and grazing at the JGOFS Sargasso Sea time series station. Deep-Sea Research I 40, 883–901.

Spall, M.A., 1995. Frontogenesis, subduction, and cross-front exchange at upper ocean fronts. Journal of Geophysical Research 100, 2543–2557.

Strass, V.H., 1992. Chlorophyll patchiness caused by mesoscale upwelling at fronts. Deep-Sea Research 39, 75–96.

Suess, E., 1980. Particulate organic carbon flux in the oceans — surface productivity and oxygen utilization. Nature 288, 260–263.

Wefer, G., 1993. Formation and composition of marine particulates. In: Heimann, M. (Ed.), The Global Carbon Cycle., NATO ASI Ser. I, Vol. 15. Springer, Berlin, pp. 505–530.

Woods, J., 1988. Scale upwelling and primary production.. In: Rothschild, B.J. (Ed.), Towards a Theory on Biological-Physical Interactions in the World Ocean.. Kluwer, Dordrecht, pp. 7–38.

Xue, H., Bane Jr., J.M., 1997. A numerical investigation of the Gulf Stream and its meanders in response to cold air outbreaks. Journal of Physical Oceanography 27, 2606–2629.

Yamamoto, T., Nishizawa, S., Taniguchi, A., 1988. Formation and retention mechanisms of phytoplankton peak abundance in the Kuroshio front. Journal of Plankton Research 10, 1113–1130.

Yoshimori, A., 1994. Horizontal divergence caused by meanders of a thin jet. Journal of Physical Oceanography 24, 345–352.